[AMERICAN JOURNAL OF SCIENCE, VOL. 294, SUMMER, 1994, P. 861–901]

LATE-STAGE ALLEGHANIAN WRENCHING OF THE SOUTHWESTERN NARRAGANSETT BASIN, RHODE ISLAND

J. P. MAHLER COGSWELL* and S. MOSHER
Department of Geological Sciences,
The University of Texas at Austin, Austin, Texas 78712

ABSTRACT. Late-stage Alleghanian deformation is broadly distributed over the western portion of the Narragansett Basin, Rhode Island, and overprints several generations of collision-related, synmetamorphic, nappe-like folds. The geometries of all structural generations are profoundly influenced by the curved western basin margin, indicating that the shape of the margin is not just an erosional feature. The late phase structures are best explained by two independent transcurrent shear zones: (1) sinistral transcurrent motion on (and between) north-northeast-striking zones in the western passage of the Narragansett Bay and along the western basin margin, and (2) dextral transcurrent motion along a wide northeast-striking zone from the Beaverhead shear zone to the western basin margin. Deformation within the high-grade metamorphic rocks in the western portion of the basin is expressed much differently than that in the lower grade rocks of the southeastern and south-central portions of the basin.

INTRODUCTION

The Alleghanian orogeny played a significant role in the evolution of the Appalachian internides (see review by Snoke and Mosher, 1989, and references therein). The orogeny was diachronous, reflecting complex plate interactions during the late Paleozoic evolution of Pangea. In New England, the orogenic effects include formation and filling of Pennsylvanian sedimentary basins (Skehan, Rast, and Mosher, 1986), upper amphibolite facies regional metamorphism synchronous with polyphase folding of the Pennsylvanian basin fill (Mosher, 1983; Murray, 1988), Carboniferous to Permian granite intrusions (Aleinikoff, Moench, and Lyons, 1985; Zartman and Hermes, 1987), disturbance of isotopic systems in basement rocks across much of southeastern New England (Dallmeyer, 1982; Zartman, Hermes, and Pease, 1988), and shear zones with thrust, normal, and/or strike-slip motion (O'Hara and Gromet, 1985; Wintsch and Sutter, 1986; Goldstein, 1989; Mosher and Berryhill, 1991; Getty and Gromet, 1992a and b). The metasedimentary rocks of the largest Pennsylvanian basin, the Narragansett Basin (fig. 1), record only Mesozoic rifting and late Pennsylvanian/Permian Alleghanian deformation and thus provide an excellent place to study the effects of the Alleghanian orogeny. The structural history of low to medium grade metasedimentary rocks from the south-central and southeastern portion of the basin has been studied in detail (numerous unpublished master's theses; results summarized in Mosher, 1983; Snoke and Mosher, 1989) and generally correlates with that for the adjacent basement (see Reck

* Present address: Exxon U.S.A., P.O. Box 4697, Houston, Texas 77210-4697.

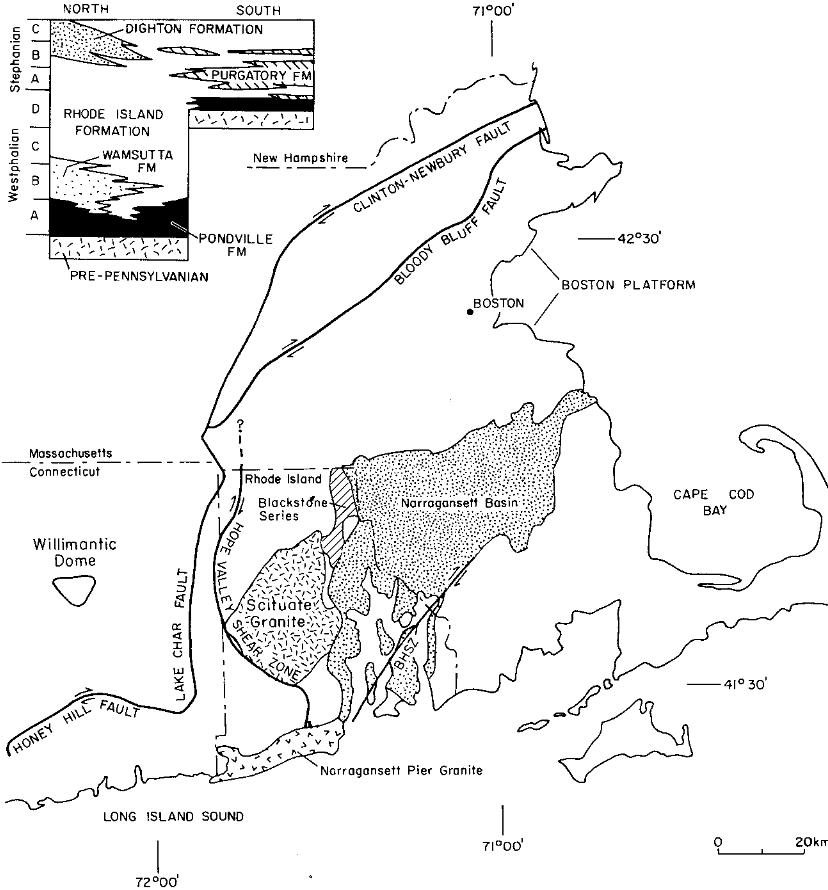

Fig. 1. Map of southeastern New England showing location of the Narragansett Basin, major faults, and units mentioned in text (adapted from Snoke and Mosher, 1989) and stratigraphic column of Narragansett Basin (after Mosher, 1983). (BHSZ—Beaverhead shear zone).

and Mosher, 1989, for discussion). Preliminary work by Mosher (1985) in the southwestern portion of the Narragansett Basin suggested that a change in deformational style and intensity occurs going from east to west across the southern portion of the basin. The present study was undertaken to characterize this change, to determine the kinematic history of the southwestern portion of the basin, and to find the relationship, if any, of the deformation of basin sediments to Alleghanian dextral motion along the Hope Valley shear zone, which lies just to the west of the basin margin (O'Hara and Gromet, 1985) (fig. 1). Recent dates on the deformational fabric within that zone (Gromet, 1991), however, indicate that motion occurred near the end of sediment deposition and is thus unrelated to the subsequent deformation of the basin sediments.

The deformational history for the study area was determined using a combination of detailed field work, thin section analysis, and geometric analysis. Kinematic indicators are rare. The three different types of evidence will be presented separately to show the data and detail used to define the changes in late-stage deformation toward the southwestern margin. Although the emphasis of this paper is on the late-stage deformation, it is necessary to document the earlier contractional deformation as well, to put the later events into a regional and temporal context.

Narragansett Basin.—The Narragansett Basin is an arcuate composite graben filled with Pennsylvanian nonmarine clastic sediments (Skehan and others, 1979; Skehan, Rast, and Mosher, 1986; Mosher, 1983) which extends offshore to the south and under Cape Cod Bay to the north (Miller, 1952; McMaster, de Boer, and Collins, 1980) (fig. 1). The formation of the basin is a result of post-Acadian tectonism. Apparent east-west extension, perhaps as a result of sinistral strike-slip motion along northeast- to east-northeast-trending faults (McMaster, de Boer, and Collins, 1980; Mosher, 1983), created a series of small grabens that coalesced to form the basin. The composite nature of the basin is evident from the extensive network of east-northeast-, north-northeast-, northeast-, and northwest-trending faults that bound horst blocks throughout the basin and from sedimentation patterns (McMaster, de Boer, and Collins, 1980; Henderson, ms). These faults were reactivated during the Permian (Henderson and Mosher, 1983; Mosher and Berryhill, 1991). Basin sediments, in general, are terrigenous clastic sediments with rapidly alternating facies ranging from alluvial fan to braided and anastomosing stream deposits (Mutch, 1968; Severson, ms) with interfingering relationships indicating lateral progradation and some vertical aggradation (fig. 1). The metasedimentary rocks unconformably overlie Cambrian marine metasedimentary rocks and Precambrian and Devonian igneous rocks and range in age from Westphalian A or B to Stephanian B or C on the basis of plant fossils (Lyons, 1984).

Methods.—The study area extends 6.8 km along the coastline, centered around the Jamestown Bridge, and 4.3 km inland, in the Wickford Quadrangle of Rhode Island (fig. 2). The basin margin is located along the western edge of the study area. In the southern part of the area, the margin trends north; farther north, the margin curves into a west-northwest orientation (fig. 2). The only formation present in the study area is the Rhode Island Formation, a meandering to braided stream deposit with rapidly changing facies that is Westphalian C in age (Lyons, Tiffney, and Cameron, 1976). The rock types include highly carbonaceous shales, quartz arenites, and coarse conglomerates with clasts up to 9 cm in length. Bedding has been transposed during deformation. The competent sandstones form boudins in the fold hinges while the less competent shales flow in between these boudins (fig. 3A). Bedding is more continuous along the fold limbs. Cross-bedding and channel lag

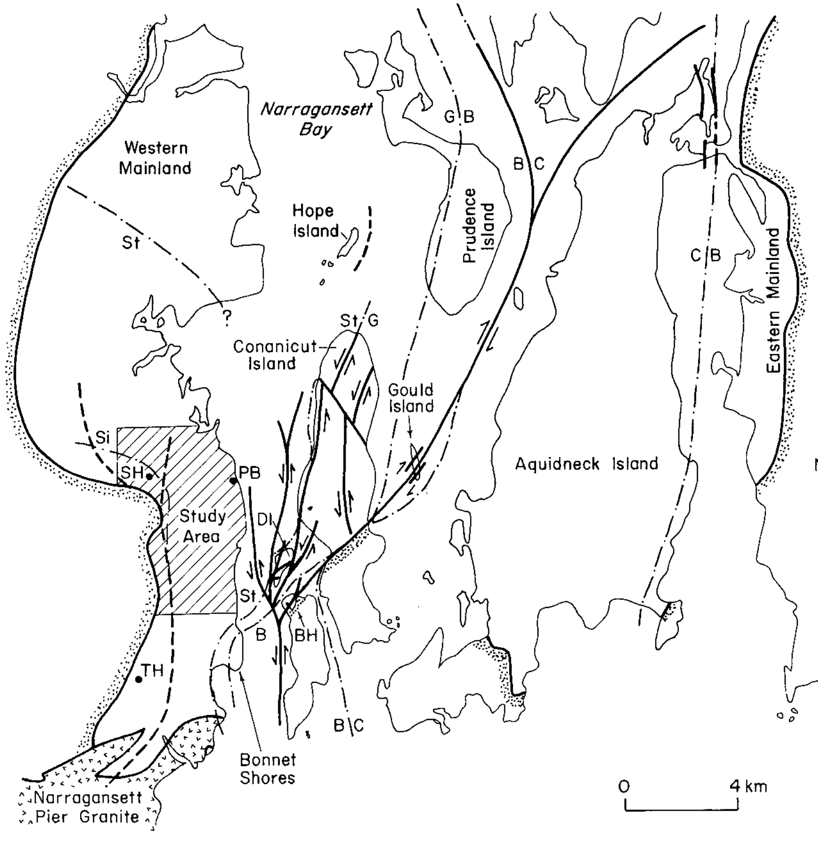

Fig. 2. Map of the southern portion of the Narragansett Basin showing structural features, isograds, and locations mentioned in text. Basin margin is stippled; study area is indicated by ruled lines. Major shear zones in western passage of the Narragansett Bay and the Beaverhead Shear zone shown with heavy solid lines; lineaments from bedrock elevation maps shown as heavy dashed lines. Isograds are commonly fault controlled and are shown as dash-dot lines where the trend diverges from that of the faults. Note that the sillimanite isograd merges with and apparently follows (southward) the lineament (dashed line) along the western basin margin. (C-chlorite, B-biotite, G-garnet, S-staurolite, Si-sillimanite) (Locations: SH—Stook Hill, PB—Plum Beach, TH—Tower Hill, DI—Dutch Island, BH—Beaverhead).

deposits, as well as rip-up clasts, are still identifiable, allowing younging (and therefore facing) directions to be determined.

The nature of the outcrop requires the type of approach used in this project. The outcrop, except on the beach, is badly weathered and overgrown with lichen, so it is difficult to determine the generation of the foliation being measured. Further, the area is intensely deformed on such a small scale that the orientations and geometric relationships of the foliations vary dramatically within very short distances. The foliations were mapped on the basis of deformational style (see below) instead of continuity of orientation, which, in retrospect, allowed for a consistent determination of generation. Outcrops are glacially rounded oblong bodies, so transects of measurements of all visible foliations were taken approx every 3 m both across and down the length of the outcrop. Oriented samples were taken at almost every measurement locality. The order of formation of the foliations was then determined from an oriented thin section and compared with the field measurements and the hand samples to get both the orientation and generation of the foliation and to work out the geometry of the folding. Ultimately, 700 oriented samples were collected, most of which were examined in hand sample and used in the analysis. A total of 250 oriented thin sections were cut to determine the generation of the foliations. The strike and dip of the foliations were plotted areally after the generation was determined from thin section and hand sample analysis (Mahler, ms). The geometric analysis included the construction of cross sections and form surface maps and calculation of fold axis orientations from 2050 strike and dip measurements (Mahler, ms). As little kinematic data are available in the southwestern portion of the basin, the results of the geometric analysis were used as constraints on various possible kinematic models.

FIELD EVIDENCE

In the present study area, two metamorphic foliations (S_{1b} and S_3) are readily observable. Both foliations are folded by open, upright folds (F_4), and the earlier of the two foliations (S_{1b}) is axial planar to a generation of isoclinal folds (F_{1b}). Folds (F_3) associated with the later foliation (S_3) and earlier generation structures (F_{1a}, S_{1a} ; S_2) are rarely observable in the field. The earliest structures (F_{1a}, S_{1a}) are poorly preserved and may be the result of either a separate or a progressive phase of deformation and hence are termed F_{1a}, S_{1a}. The structures observed in the field will be discussed in order of formation, although much evidence for the relative timing and presence of the structures comes from thin sections.

Only two F_{1a} folds are observed in the field: (1) a folded quartz vein refolded by an F_{1b} fold, and (2) a mesoscopic, isoclinal fold defined by a deformed conglomeratic layer within a sandstone. The latter fold is an F_{1a}, because S_{1b} is neither deformed nor axial planar to the fold; instead it cuts the fold. S_{1a} can be seen in the field, though it is difficult to identify as such without a thin section. In the field, S_{1a} is similar to the later S_3 foliation, because it is faint and defined by aligned micas or ductilely deformed clasts that are not as obviously elongate as those of S_{1b}.

F_{1b} and S_{1b} are the most readily observable generation of structures in the field. Folded cross-bedding, which changes from right side up to upside down within a distance of 1 m, commonly defines the folds. The cross-bedding is clearly asymptotic at the basal bed boundary and erosionally truncated at the upper bed boundary so that the younging direction is identifiable. As a result of this folding event, bedding frequently is

A.

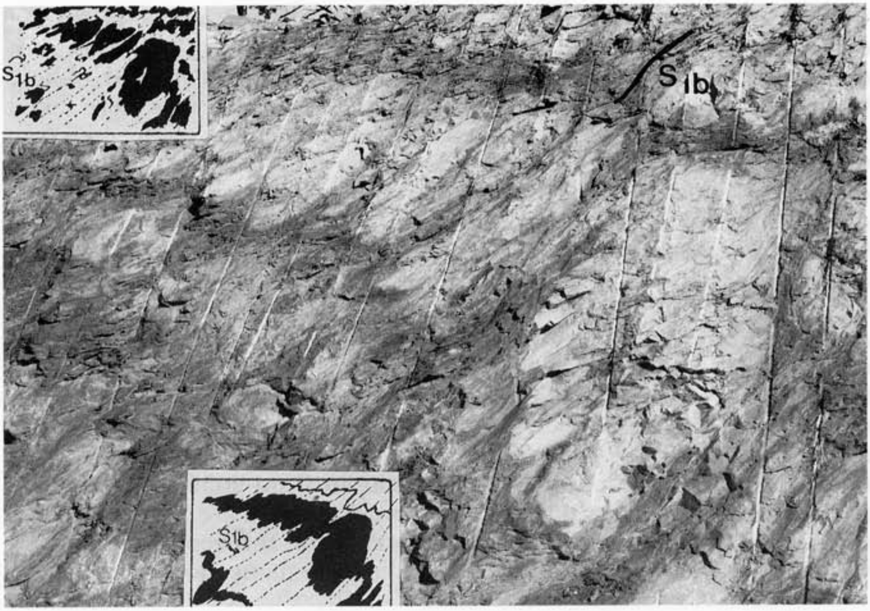

B.

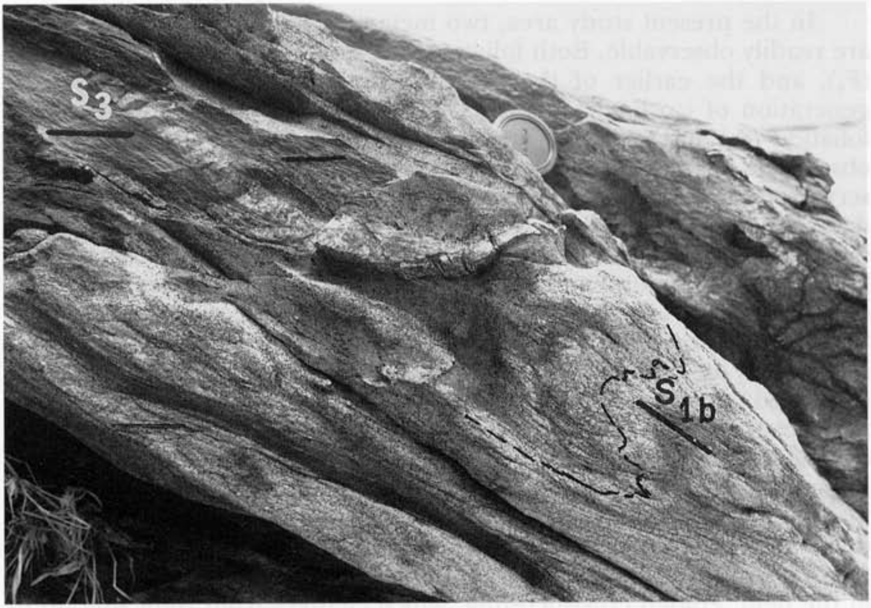

Fig. 3(A) Asymmetric, west-verging F_{1b} fold defined by light-colored sandstone layers in black phyllite. Pronounced axial planar foliation is S_{1b}. Sandstone layer has been pulled apart to form boudins or pods surrounded by darker phyllite. The long dimensions of the pods lie within the axial surface of the fold. In upper sketch of outcrop, the most distinctive individual pods are shown. In lower sketch, pods are connected to show original continuity of sedimentary layers. S_{1b} is dashed in both. Photograph taken of vertical roadcut on Route 138 just north of Plum Beach, facing south. Nearly vertical drill holes are about 6 cm in diameter.

transposed in the fold hinges. The more competent sandstones, interlayered with the ductile shales, form boudins or lens-shaped "pods" in the hinge region of the folds (fig. 3); whereas on the limbs, the beds maintain their continuity. In the hinges, the less competent shale has flowed between these pods, so the apparent sandstone/shale contact is not a true bedding orientation. The long dimensions of the pods lie within the axial surfaces of the folds, and the hinges of the folds are recognizable by connecting the groups of pods. In thin section, these structures fold a metamorphic foliation (S_{1a}). The earliest pervasive foliation visible in the field, S_{1b}, is axial planar to these folds (fig. 3). It is defined by ductilely deformed, elongate quartz grains and by aligned micas in the finer grained rocks. In coarser grained sediments, pebbles and cobbles are aligned parallel to S_{1b} and are elongate parallel to F_{1b} as well. Ductilely deformed, elongate quartz is distinctive and is characteristic of the deformational style used to trace the foliation across the study area where folds are not visible. Within the schists, S_{1b} is axial planar to small floating intrafolial fold hinges of quartz veins that lie between S_{1a}. A biotite lineation trending and plunging northeast occurs frequently on the S_{1b} surface and is probably associated with F_{1b}, as are the elongate cobble and quartz clasts.

In this study area, there are two or three superposed, noncoaxial crenulation cleavages affecting the S_{1b} surface in some locations. The cleavages commonly affect only part of an outcrop and are localized in generally north-trending zones. In thin section, some of these crenulations are affected by the S_3 foliation (and thus are S_2), and some are not, suggesting more than one generation may be present. The relationship of these cleavages to other structures is difficult to determine, because there are not enough at any locality to see whether they remain constant with respect to F_4 (and are related) or whether they are reoriented by F_4 (and formed earlier). The trend and plunge of crenulation axes on the S_{1b} surface and the trend and plunge of the F_3 and F_4 fold axes were all plotted on the same stereonet for each crenulation locality. None of the crenulations clusters around F_3, and, in the majority of cases, the crenulations show no relationship to F_4. If the crenulations cluster around the F_4 fold axis, they are considered related to F_4. If they do not, they are considered unrelated to F_4 and probably represent S_2. The probable S_2 crenulation cleavages generally trend north-northwest to north-northeast and, where more than one are superposed, usually young in a clockwise direction.

Fig. 3(B) Close-up of individual sandstone pods or boudins from hinge region of large F_{1b} fold showing internal structures. Boundaries of pods are diffuse. Pronounced metamorphic foliation is S_{1b}. Pod on lower right contains parasitic folds. (Center of one layer is dashed.) Note other folds, internal podding of layers and floating hinges in lower right corner. Both bedding and S_{1a} are folded by these folds. S_{1b} is a crenulation cleavage of S_{1a}. A faint S_3 cuts across the outcrop at a shallow angle; the interference of S_{1b} and S_3 forms a diamond-shaped weathering pattern. (Three shallow dashes indicate places where S_3 is visible in photograph.) Taken at Plum Beach, facing north, a 6 cm lens cap for scale.

In the field area, the second predominant foliation is S_3 (fig. 3B). No F_3 hinges were recognized in the field, though they must be present because the angular relationship between S_{1b} and S_3 changes over short distances throughout the area. The F_3 folds should fold bedding, S_{1a} and S_{1b}. S_3 is a pervasive and penetrative foliation defined by aligned muscovite and biotite. The tails of sand pods, conglomerate cobbles, and ductilely deformed, elongate quartz grains of S_{1b} curve into parallelism with S_3. Little or no elongate quartz is associated with S_3, which helps distinguish S_3 from S_{1b}. Additionally, the spacing between individual S_3 foliation planes is generally larger than that between S_{1b}.

The other readily visible fold generation (F_4) in the field area is large, open folds of S_{1b} and S_3. These fold axes can be measured directly in the field, along the beach, and generally trend near N40°E. No axial planar foliation is associated with F_4, but, on the basis of the stereonet calculations used to distinguish crenulation cleavage generations, some crenulations are roughly coaxial with F_4. The F_4 folds are deformed by boudinage with north-south extension and a down-to-the-north sense of motion. These boudins are completely exposed in coastal outcrops. In the poor exposures in the woods they are also visible but are more difficult to identify as such.

THIN SECTION ANALYSIS

Structural petrology.—Thin sections were used to confirm or determine the generation of structure seen in the field. Overall, five foliations are identifiable in thin section: S_{1a}, S_{1b}, and S_3 fabrics, S_2 and S_4 crenulation cleavages; however, in most thin sections, only two or three are visible. The appearance of the foliations varies with the lithology, although the mineral assemblages defining the foliations are essentially the same. Despite the degree of metamorphism and deformation, detrital grains and clasts can be distinguished within sandstone units. Flattened quartz and quartz/feldspar, sand-size clasts are rimmed by micas, pinning the original boundaries. Detrital quartz and feldspar grains, outlined by micas or graphite, are preserved as cores of larger grains. Very large muscovite plates also appear to be detrital. Similar muscovite plates with ragged edges are observed in sandstones at chlorite and lower grades within the basin; with increasing metamorphic grade, the edges become progressively less ragged. In some arkosic samples at the highest (sillimanite) grade, the large plates are also very ragged as a result of chemical breakdown.

S_{1a}, when present, is defined by ductilely deformed, elongate quartz clasts, aligned so that the edges of the clasts are parallel to the foliation, or it is defined by an early generation of very large, apparently detrital, muscovite plates (fig. 4). S_{1a} is generally parallel to bedding. The foliation is overgrown, cut, or wrapped by S_{1b} and S_3. In places, S_{1a} has been crenulated to form S_{1b}. In such cases, the large muscovite plates that define S_{1a} are often pulled apart by extension parallel to S_{1b}.

A.

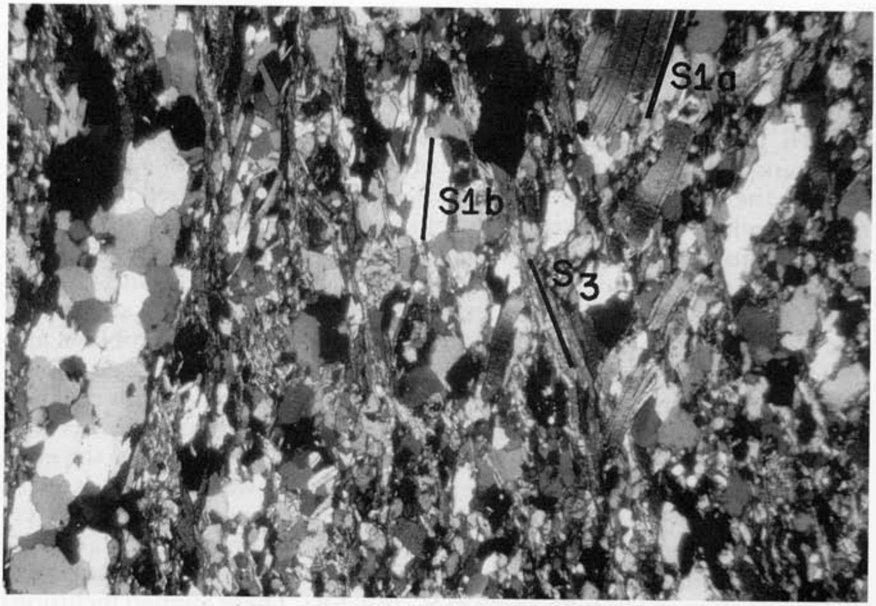

B.

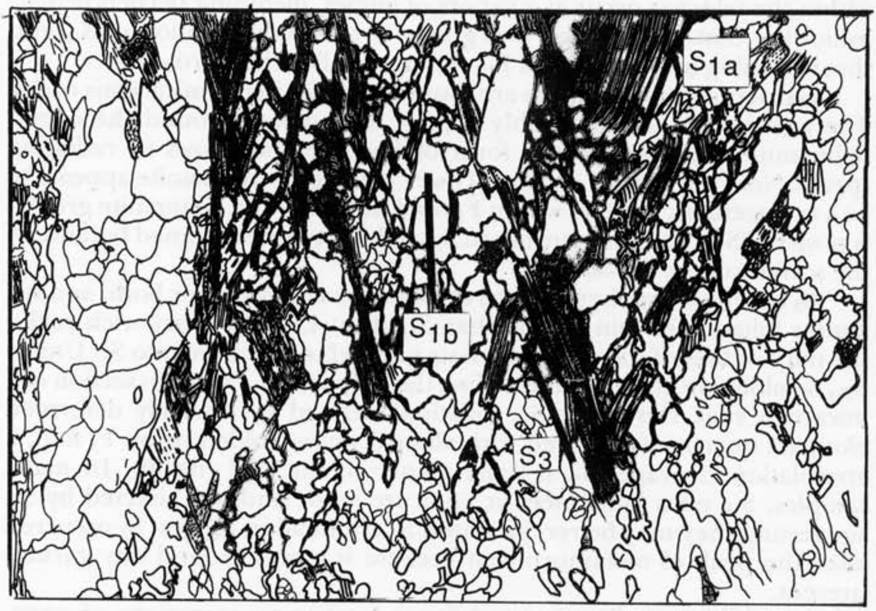

Fig. 4. Sandstone with three foliations visible. S_{1a} is defined by large aligned muscovite plates. S_{1b} is vertical and is defined by elongate quartz clasts and grains and fine-grained micas. S_3 is defined by aligned small muscovite and biotite laths. (A) Photomicrograph (measures 1.2 cm across, crossed polars). Orientation of foliations indicated; minerals defining the three foliations are observable in these orientations across the entire photomicrograph. (B) Sketch of photomicrograph.

The earliest dominant foliation, S_{1b}, is characteristically defined by ductilely deformed, elongate quartz grains and aligned biotite and muscovite (figs. 4, 5, and 6). The long edges of the grains are aligned parallel to the foliation, or, if it is a quartzite clast, the edges of the clast are aligned parallel to the foliation, but the internal quartz grains and subgrains are either unoriented or oriented parallel to an earlier foliation. In the highly micaceous rocks, S_{1b} is defined by aligned biotite and muscovite laths and is axial planar to floating intrafolial fold hinges of very fine quartz veins, which probably formed along the earlier S_{1a}, and to folds of bedding defined by concentrations of biotite and opaque minerals. Mica laths meet at acute angles bisected by S_{1b}, suggesting recrystallized crenulation hinges. Inclusion trails in porphyroblasts also indicate that S_{1b} is a crenulation of S_{1a}. Staurolite, garnet, and biotite porphyroblasts show sigmoidal inclusion patterns; the inclusion trail is at a high angle to the S_{1b} foliation in the crystal centers and curves into parallelism with S_{1b} on either end (fig. 5A). Pressure shadows on the ends of the porphyroblasts are parallel to S_{1b} and are warped by a later S_3 foliation. This evidence suggests that staurolite, garnet, and biotite overgrew the S_{1a} foliation, as it was being crenulated to form S_{1b}. Large albite and microcline porphyroblasts are elongate parallel to S_{1b} but have inclusions aligned at a high angle to S_{1b} (fig. 5B). These aligned inclusions within the feldspar occur at a variety of angles, including perpendicular, indicating that the feldspar overgrew a crenulation foliation of S_{1a} and that flattening associated with F_{1b} continued after their growth.

Garnets and rare kyanite are found along S_{1b} in the micaceous rocks. The garnets are usually highly altered to hematite around the edges. Sillimanite is present in the form of fibrolite and grows in radiating sprays. Near the granite contact (Tower Hill; fig. 2), sillimanite appears to be a replacement mineral within F_{1b} fold hinges. Thus, sillimanite growth is post-F_{1b}/S_{1b}. The relationship to S_3 could not be determined because of the scarcity of the fibrolite.

S_3 is defined by aligned laths of biotite or muscovite, or both, and is a fainter foliation in thin section than S_{1b} (figs. 4, 6). In quartz-rich rocks, the narrow tails of the elongate clasts parallel to S_{1b} curve into S_3. Unlike S_{1b}, no elongate quartz grains define the S_3 foliation. One thin section of a mica-rich rock shows the S_{1b} foliation, defined by ductilely deformed elongate quartz interlayered with aligned micas, folded by an F_3 fold; a crenulation cleavage, S_3, is axial planar to the fold (fig. 6). In many samples, S_{1b} mica laths meet at an acute angle and are bisected by S_3, suggesting they may be recrystallized S_3 crenulation hinges. S_3 occurred after the peak of metamorphism because it wraps around any garnets present.

In addition to S_{1a}, S_{1b}, and S_3, at least two generations of open, undifferentiated crenulation cleavages are visible in both micaceous and quartz-rich rocks. Micas in the hinges are both bent and recrystallized, with most recrystallization occurring in tight, kink-like crenulations. These crenulations are either S_2 or S_4. Both S_2 and S_4 are sets of

A.

B.

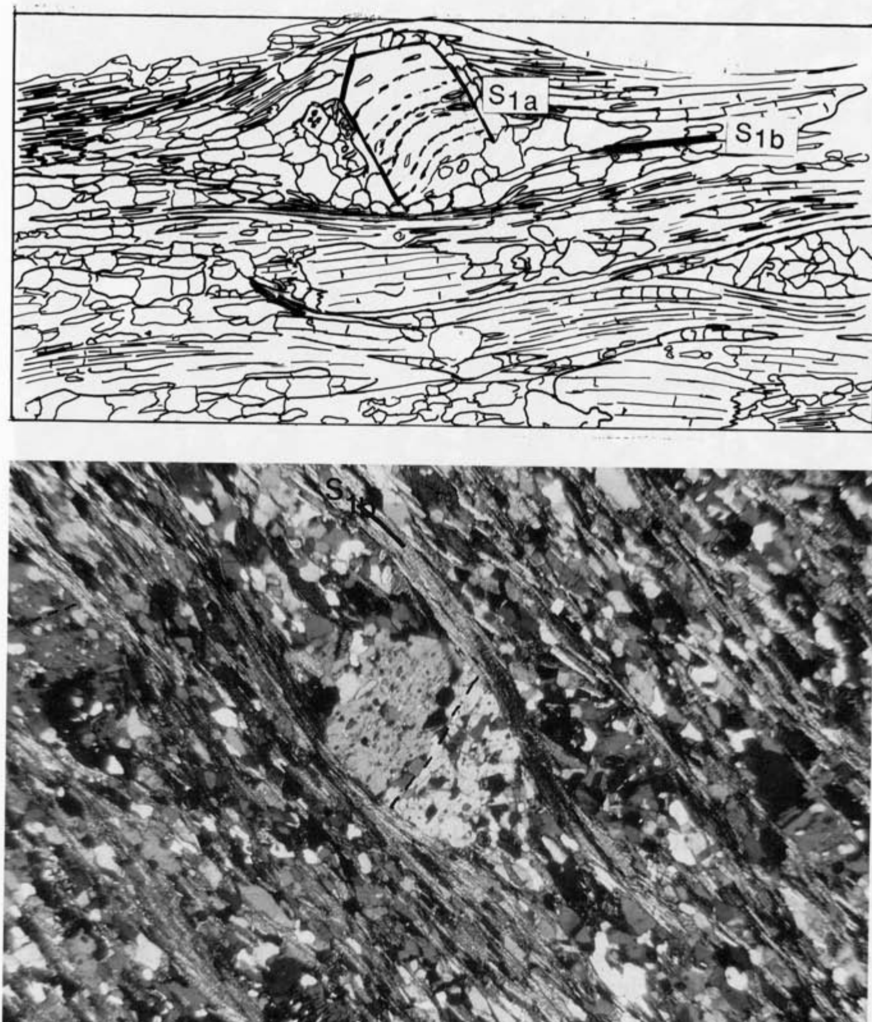

Fig. 5. Porphyroblasts with aligned inclusions parallel to S_{1a}. Predominant foliation, S_{1b}, is defined by aligned micas, elongate quartz grains, and pressure shadows off the porphyroblasts. (A) Sketch of photomicrograph. Staurolite with sigmoidal inclusion pattern indicating that staurolite grew syntectonic to S_{1b} and that S_{1a} was crenulated to form S_{1b}. (Sketch measures 1.2 cm across.) (B) Photomicrograph of microcline porphyroblasts. Microcline is elongate parallel to S_{1b} and contains straight inclusion trails in different orientations, indicating that it overgrew a crenulated foliation of S_{1a} and that flattening associated with S_{1b} continued after its growth. Orientation of inclusion trails (parallel to S_{1a}) indicated for two porphyroblasts (center and far left). Note other smaller porphyroblasts with inclusions also oriented at high angles to S_{1b}. (Photomicrograph measures 5 mm across, crossed polars.)

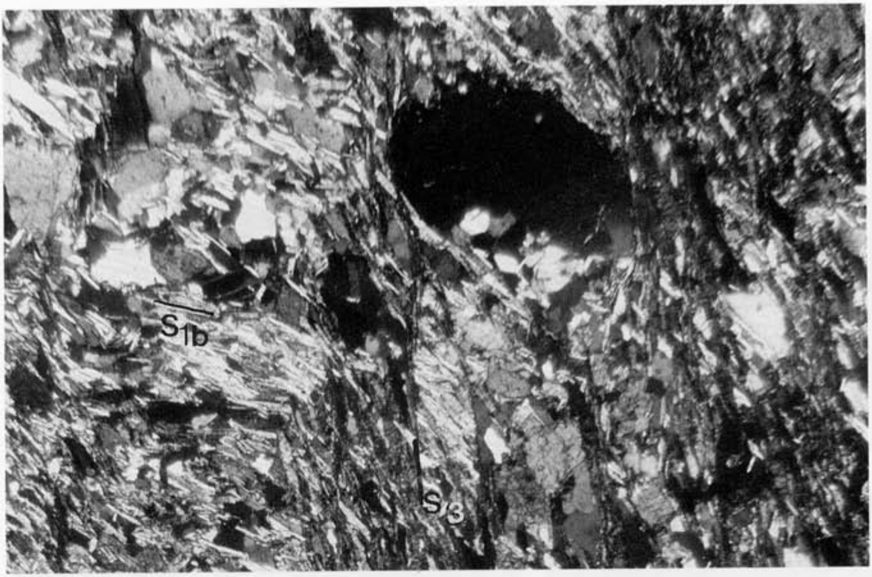

Fig. 6. S_{1b} foliation crenulated to form S_3 (vertical foliation). Muscovite and elongate quartz define S_{1b}; S_3 is defined by crenulation limbs and new metamorphic muscovites that are oblique to and overgrow S_{1b}. Large feldspar porphyroblast (dark, upper center) shows faint quartz inclusions parallel to S_{1a} that are oblique to both S_{1b} and S_3. (Photomicrograph measures 3.3 mm across, crossed polars.)

superposed, noncoaxial crenulations, so early versus late cannot be determined simply from cross-cutting relationships of the crenulations themselves. In a few places they can be distinguished by their relationship to S_3. S_2 crenulations are apparently partially overgrown by S_3, whereas S_4 crenulates S_3. S_4 crenulations have a tendency to form box folds with offset of the limbs and pressure solution along the axial planes. S_2 can form a pronounced crenulation cleavage with associated pressure solution resulting in quartz-rich hinges and mica-rich limbs. A late-stage pressure solution cleavage, unrelated to S_2 or S_4, is also observed. It usually parallels and reactivates S_{1b}, but in some locations it follows S_3.

In summary, the earliest foliation visible is S_{1a}, defined by elongate quartz or large muscovite plates. Orientation of the muscovite plates and inclusion patterns in garnet, biotite, staurolite, and feldspar indicate S_{1a} was crenulated to form S_{1b}. S_{1b} is defined essentially by ductilely deformed, elongate quartz grains and aligned muscovite and biotite. S_3 overgrows and crenulates S_{1b} and is defined by aligned muscovite and biotite. S_2 and S_4 are undifferentiated, open crenulations deforming S_{1b} or S_{1b} and S_3.

Metamorphism.—The study area and the basin as a whole have undergone two phases of metamorphism: an early Barrovian phase (M_1) and a later retrograde phase (M_2). The shale units are typical pelites with metamorphic assemblages including sillimanite, kyanite, staurolite, garnet, muscovite, and biotite, as well as chlorite and sphene. The first Barrovian phase reaches sillimanite grade in the southwestern portion of the study area and changes to staurolite grade progressively northward, reaching biotite grade outside the study area to the northeast. The sillimanite isograd curves from north-trending parallel to the coastline to east-trending in the northern portion of the area, following the curved trend of the southwestern basin margin (fig. 2).

Two previous studies (Grew and Day, 1972; Jones, ms) have estimated the pressure and temperature conditions of metamorphism through petrographic analysis of samples at Stook Hill (fig. 2). Both found sillimanite, kyanite, staurolite, garnet, and biotite coexisting at this site and concluded that the kyanite and staurolite, with muscovite, biotite, and quartz, formed an equilibrium assemblage. Jones (ms), using microprobe data, found temperatures must have exceeded 600°C and pressures reached 6.5 kb. He attributes the presence of sillimanite to decompression during rapid uplift which shifted metamorphism from the kyanite to the sillimanite stability field. Grew and Day (1972), however, postulate that contact metamorphism during intrusion of the Narragansett Pier Granite caused replacement of staurolite by sillimanite and muscovite. If so, this would represent an additional phase of metamorphism.

Although a detailed metamorphic analysis was outside the scope of this study, the following observations were made during the structural analysis of about 250 thin sections. Both kyanite and sillimanite (as fibrolite) are very rare, and extensive retrograde alteration obscures the original mineralogy of many samples. Over the entire area, biotite commonly alters to chlorite and feldspar to sericite. Many samples contain abundant, large, altered porphyroblasts which cannot be identified optically. At Plum Beach, three samples show undeformed psuedomorphs containing biotite, muscovite, garnet, feldspar, and quartz. In most samples, however, the main Barrovian phase mineral assemblages are preserved. Throughout the area, large biotite and muscovite blades appear in textural equilibrium. Although staurolite is present everywhere, it is only moderately abundant. It is best preserved in the arkosic (mica-poor) rocks and is partially altered to biotite and/or muscovite. Where observed at Stook Hill, fibrolite showed no relationship to staurolite. Near the Narragansett Pier Granite contact at Tower Hill (fig. 2), abundant sillimanite and muscovite and lesser amounts of chlorite form psuedomorphs of large porphyroblasts that have the morphology of staurolite. Grew and Day (1972) observed relict staurolite within these large psuedomorphs. Smaller biotite porphyroblasts have been retrogressed to chlorite. The abundance of sillimanite near the granite contact and the lack of similar replacement textures farther away suggest localized contact metamorphism, as suggested by Grew and Day (1972). Another cause, such as rapid decompression, as proposed by Jones (ms), seems most likely for the rest of the area; however, the observations made in this study do not constrain the cause of this later sillimanite growth.

The location of the sillimanite isograd in figure 2 should be considered approximate. It marks the northernmost and easternmost occurrence of confirmed sillimanite (Grew and Day, 1972; Jones, ms; this study). The eastern boundary is questionable as samples from coastal outcrops within the study area from Plum Beach south contain radiating sprays of needles strongly resembling fibrolite. Although the sprays occur rarely within quartz, feldspar, and biotite, most occurrences are within porphyroblasts of retrograde chlorite. High relief, low birefringent relicts (too corroded and small to identify optically) within the chlorite suggest that the preexisting porphyroblast was not biotite. The needles, if once sillimanite, may have been replaced by white mica. If these are or were fibrolite, the isograd lies farther east parallel to the coastline in the western passage of Narragansett Bay (fig. 2). The outcrops on the western coastline of Conanicut Island are staurolite grade rocks. The east-trending segment of the sillimanite isograd, which lies just north of Stook Hill (and Plum Beach if the north-trending segment lies farther east), is better constrained on the basis of lower grade assemblages and the lack of any questionable relict mineralogy. For example, just north of Stook Hill, microcline porphyroblasts overgrow S_{1a} and parallel S_{1b}. If these rocks were at sillimanite grade, the most likely K feldspar to grow would have been orthoclase. This observation is supported by textural relationships at Stook Hill where some of the arkosic samples show large muscovite blades in textural disequilibrium with feldspar. Although the same rocks show later alteration of feldspar to sericite, it appears that the large muscovite blades are breaking down to form orthoclase, suggesting temperatures approaching the second sillimanite isograd. A careful metamorphic analysis across the entire area is needed to unravel the complex metamorphic history and location of isograds.

The timing of the main Barrovian phase is constrained by several pieces of evidence. Metamorphism began during the formation of S_{1a}, reached its peak during and after S_{1b} formation, and continued through the formation of S_3. Ductilely deformed quartz defines S_{1a}, indicating metamorphism had started by the time S_{1a} formed. The garnets growing along S_{1a} and the staurolite and feldspar porphyroblasts overgrowing S_{1a} (as indicated by the inclusion patterns) all indicate that the peak of metamorphism postdated S_{1a}. S_{1b} is defined by metamorphic biotite and muscovite laths. The sigmoidal pattern of the inclusions in staurolite, garnet, and biotite and the pressure shadows parallel to S_{1b} indicate that those minerals are probably syntectonic to S_{1b}. The feldspar porphyroblasts contain straight S_{1a} inclusion trails and are aligned parallel to S_{1b} indicating syn-S_{1b} growth. Kyanite and garnet grow along and overprint S_{1b} as well, suggesting that these highest grade metamorphic minerals formed, at least in part, post-S_{1b}. Metamorphic recrystallization was still occurring during S_3, as the foliation is defined by muscovite and biotite laths and recrystallized crenulation hinges. S_3 wraps around garnet, staurolite, and feldspar porphyroblasts, and pressure shadows of the staurolites are bent into S_3, indicating that S_3 formed after the peak of metamorphism. Sillimanite, where observed, forms sprays at angles to S_{1b} and appears as a replacement mineral in the center of F_{1b} hinges at Tower Hill. Thus, sillimanite growth occurred after the formation of F_{1b}/S_{1b}. The rarity of sillimanite precludes determining its relationship to S_3.

The retrograde metamorphic event postdated growth of peak metamorphic minerals but is otherwise poorly constrained. In some thin sections, the chlorite appears fresh and undeformed, whereas in others the chlorite has been kinked by crenulations. Thus retrograde metamorphism started, at least locally, before the end of deformation. Murray and Mosher (1984) suggest this retrograde metamorphism was caused by fluid movement along faults.

GEOMETRIC ANALYSIS

After determining the correct generation of the field measurements from the thin sections, the 2050 strike and dip measurements were plotted on stereonets and maps (Mahler, ms) and were used to construct cross sections and form surface maps and to calculate fold axes. Stereonets (fig. 7) show S_{1b} and S_3 dip north in the western part of the area adjacent to the west-northwest-trending basin margin (fig. 7A, E) and dip east along the southern coastline where the basin margin is north-trending (fig. 7C, G). Along the northern coastline, between the two dip domains, dips are predominantly northeast (fig. 7B, F). S_{1b} is generally

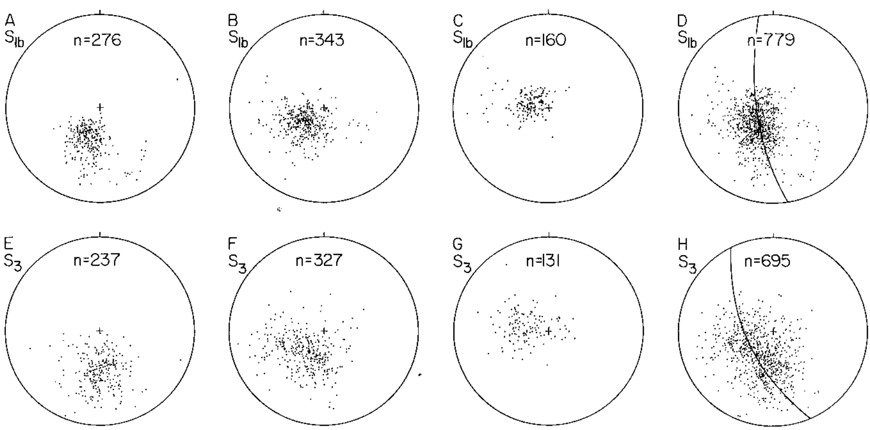

Fig. 7. Stereonets of poles to S_{1b} and S_3 for different locations across the study area. A, E: western portion of study area near Stook Hill between Route 138 and Hamilton-Allen (H-A) Road (see inset in fig. 9 for locations). B, F: northeastern portion of study area near Route 1A and northern coastline near Plum Beach. C, G: southeastern coastline. D, H: data for entire area with a best fit great circle shown. These and all other stereonets are lower hemisphere, equal angle projections.

slightly shallower than S_3. On combined plots for the entire area (fig. 7D, H), S_3 poles suggest northeast-trending F_4 folds affected the area. S_{1b} poles, which reflect the effects of both F_3 and F_4, fall on a girdle with a more easterly trending axis.

To construct the cross sections, the data along the line of section were plotted, and the deformations were removed sequentially, from youngest to oldest. Although these cross sections are not completely accurate as strain data are not available, they are good approximations and at a minimum show the style of deformation. S_{1b} and S_3 were plotted (fig. 8A), which showed the position of F_4 folds. Then S_3 was rotated to a constant dip across the section (fig. 8B), removing the F_4 folds, and the S_{1b} measurement was rotated the same amount. F_3 fold hinges were delineated by the change in the relationship between S_{1b} and S_3, just as fold hinges can be determined by bedding/cleavage relationships in less complexly deformed areas. Both foliations (and F_3 folds) were then rotated back to their original position (fig. 8C). The east-west cross section (fig. 9A) is a composite of shorter cross sections taken through the densest sections of data. About 250 data points define the folds on the east-west cross section. Both north-south and east-west cross sections are shown. These sections are not perpendicular to most fold axes, because their placement is constrained by the location of data. In any case, fold axes vary across the area making it impossible to construct a regional cross section perpendicular to fold axes.

The F_4 folds on the cross sections are defined by the S_3 foliation. The same open, large-scale folding visible in outcrop is shown on the cross sections; however, F_4's form box folds that were not apparent in the field. These box folds become tighter and have a shorter wavelength toward the western edge of the study area (box fold is used as a descriptive, morphological term). On the north-south cross section (fig. 9B), the F_4 folds show up as northward-dipping monoclinal features, because the F_4 fold axes are roughly parallel to the cross section.

From the cross sections, the F_3 folds are open to isoclinal, nearly upright to recumbent folds that are both tightened and opened by later F_4 folding. Around Stook Hill, the F_3 fold axes trend roughly east, so the east-west cross section gives an oblique view of the folds. On the north-south cross section (fig. 9B), the slightly tighter and more intense appearance around the southern end of Plum Beach is partially caused by the oblique view as the fold axes trend northeast in that locality. The cross sections suggest that the dip of S_3 in different areas (fig. 7) reflects the present F_3 vergence: westward along the coastline and southward inland; however, the original folds may have been symmetrical. It is unlikely that they verged in another direction, given their present orientation and the open nature of the F_4 folds. The shape of the F_3 folds suggest that they are small parasitic folds on a larger F_3. The synformal hinge at the west end of the east-west cross section (fig. 9A) is probably part of this larger fold.

Rudimentary cross sections showing F_{1a} and F_{1b} (fig. 10) were constructed using the limited bedding and facing data available. The

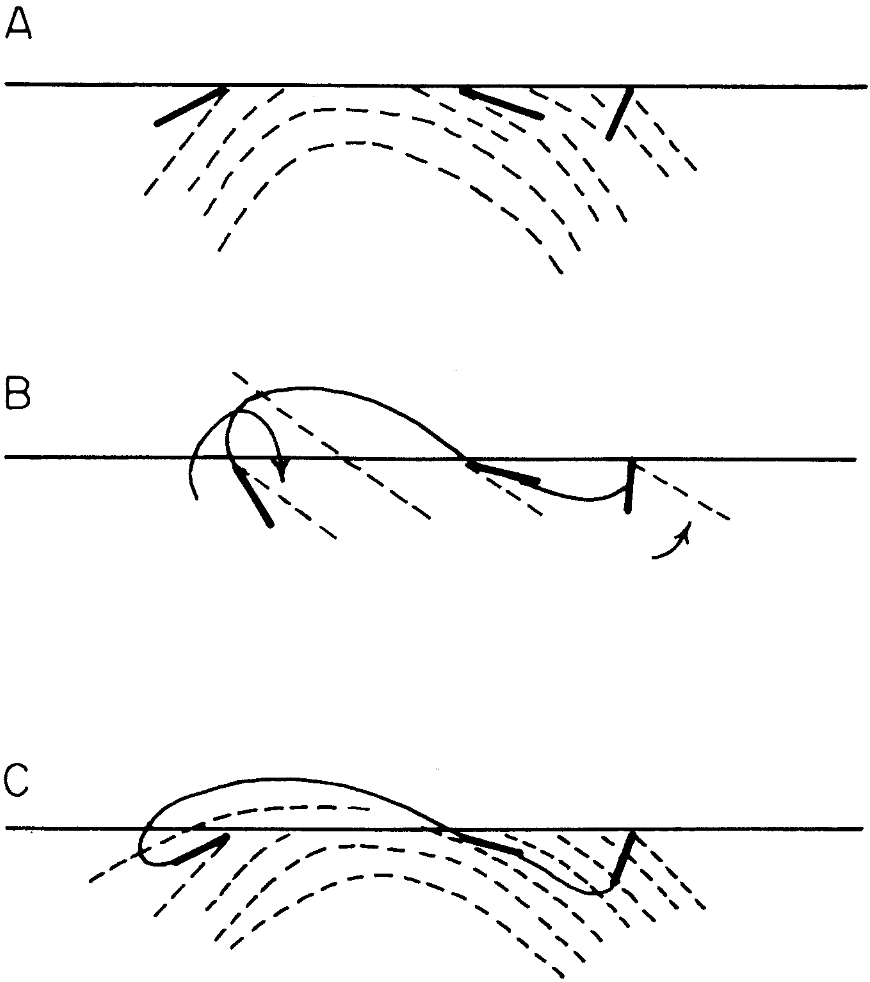

Fig. 8. Illustration of cross-section construction. (A) F_4 folds defined by S_3. S_{1b} (heavy solid line) and S_3 (dashed line) plotted (apparent dips used with strikes not perpendicular to section line). (B) S_3 is rotated to a constant dip, and S_{1b} is rotated by the same amount. Direction S_{1b} was rotated as indicated. F_3 hinges are identified by the change in relationship between S_{1b} and S_3 from clockwise to counterclockwise (or vice versa). Hinges have been sketched. (C) Data and F_3 rotated back to original orientation.

east-west cross section was constructed by performing the rotations in two steps. First, S_3 was arbitrarily rotated to vertical, rotating S_{1b} and S_0 by the same amount, to remove the effects of F_4 folds. This rotation assumes that the axial plane of F_3 was originally vertical. (Any orientation would work; the end result is independent of this assumption.) Then the S_{1b} was rotated to a constant dip across the section, rotating S_0 again as

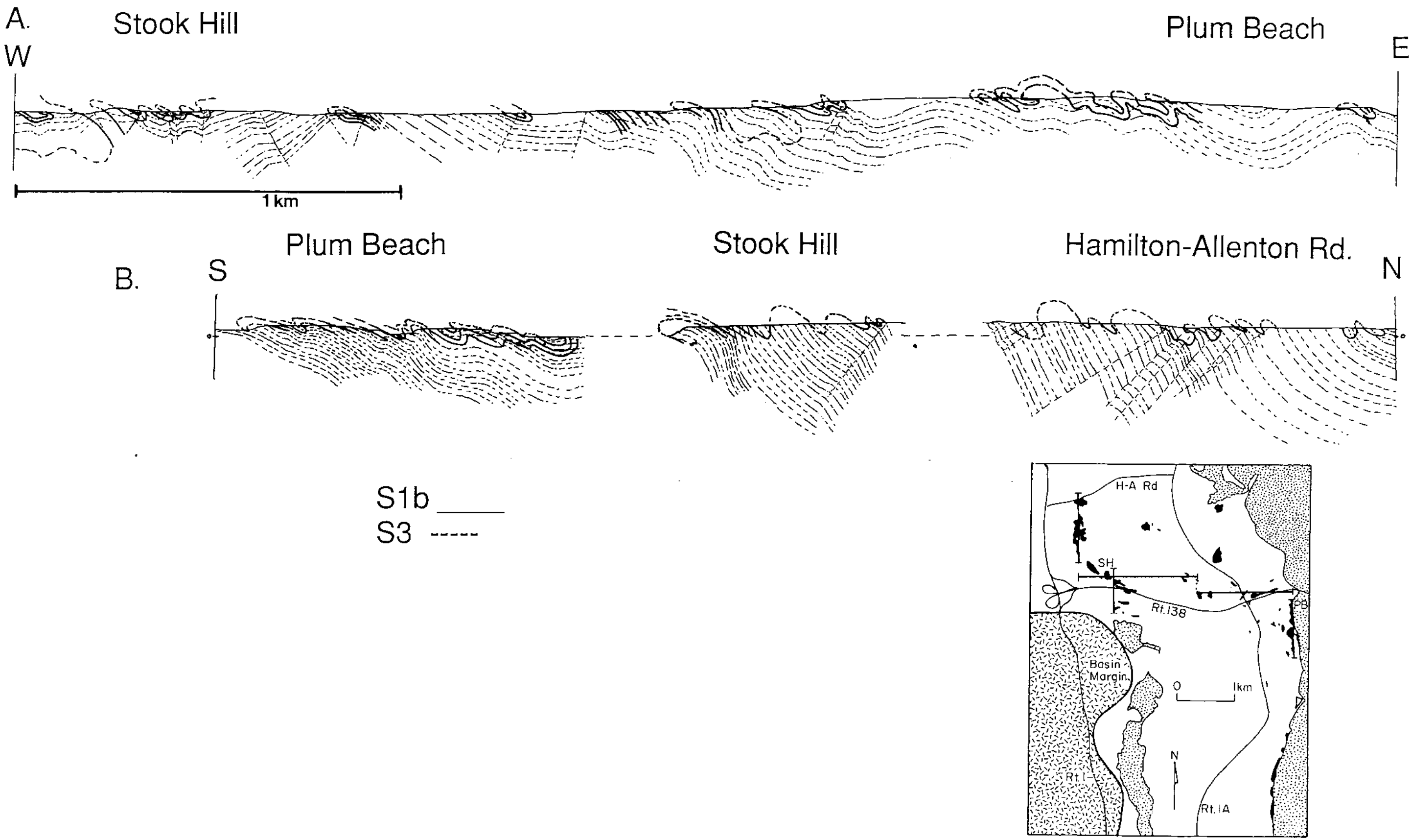

Fig. 9(A) Composite east-west cross section showing isoclinal, recumbent, west-verging F_3's refolded by F_4 box folds. (B) North-south composite cross section showing isoclinal, recumbent S-verging F_3's. (Dashes indicate break in section.) F_4 appear as north-dipping monoclines because fold axes are parallel to the cross section. Inset map shows amount of outcrop (solid black) and location of cross sections. (Basement—random dashes; water—stippled. H-A Road—Hamilton-Allen Rd., SH—Stook Hill, PB—Plum Beach.)

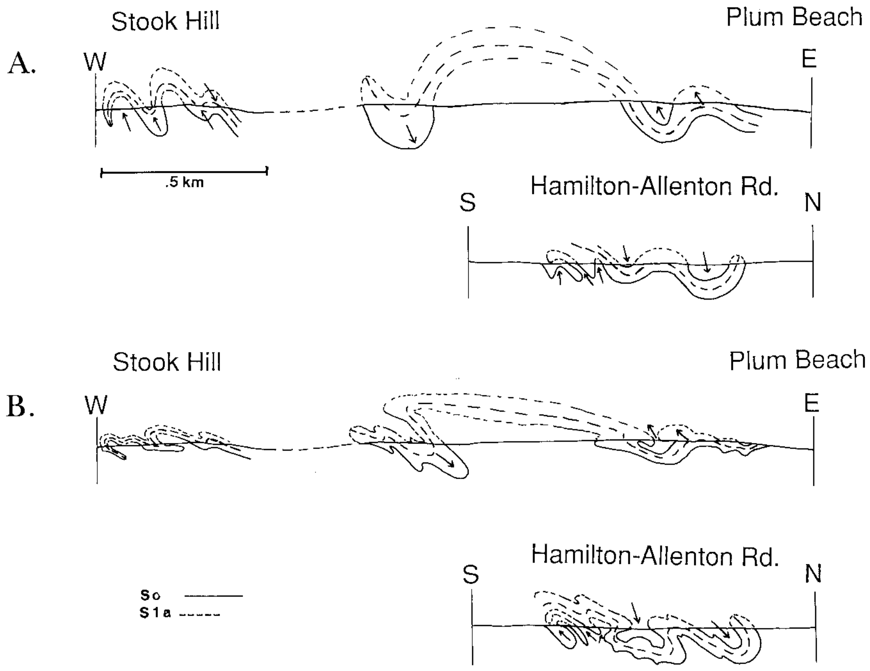

Fig. 10(A) East-west and north-south cross sections of F_{1a} and F_{1b} with F_3 and F_4 removed. Shows F_{1a}'s are large-scale, isoclinal, recumbent folds with smaller parasitic folds on the limbs. F_{1b}'s are shorter wavelength, isoclinal folds. Arrows indicate sedimentary younging directions. (B) East-west and north-south cross sections of F_{1a} and F_{1b} in current orientation refolded by F_3 and F_4. Arrows indicate younging directions. (A, B) Sections are the same scale, and section lines are the same as in figure 9; topography is dashed where part of the section is omitted due to lack of data.

well, to remove F_3. A change in angular relationship (for example, counterclockwise to clockwise) between S_{1b} and S_0 indicates an F_{1b} hinge, and a change in facing direction between folds indicates that an F_{1a} axial trace has been crossed. The blank spots on the cross section (dashed topography) are due to lack of outcrop and data.

Both the east-west and north-south cross sections, with F_3 and F_4 removed, show that F_{1a} folds are large-scale isoclinal folds that have been refolded by F_{1b}'s of a shorter wavelength (fig. 10A). Both generations of folds are recumbent, nappe-like structures that, coupled with upper amphibolite facies metamorphic conditions, suggest the deep-seated features of a collisional orogen. The same fold configuration outcrops just south of the study area (Mosher, Burks, and Reck, 1987; Reck and Mosher, 1989). The north-south cross section shows some parasitic F_{1a} folds that have been refolded by F_{1b}. Figure 10B shows the early folds rotated back to their current orientation. Superimposing F_3 and F_4 on the early deformation creates a complex interference pattern that tends to obscure the large scale and intensity of the early deformation.

Form surface maps for bedding (S_0) and foliations (S_{1a}, S_{1b}, S_3) were also constructed to help determine the nature of the deformation in the basin. The form surface maps show the trace of a penetrative foliation on the Earth's surface and were created by connecting the strike lines of the strike and dip data. The resultant map shows the fold shapes projected onto a horizontal surface. The combination of form surface maps and cross sections gives a three-dimensional view of the folds. Form surface maps for S_{1b} and S_3 are shown in figures 11 and 12, respectively. Calculated F_3 and F_4 fold axes (see below) have been superposed on the S_{1b} and S_3 form surfaces. A common feature of both form surface maps is that the surface always trends parallel to the curved basin margin, as does the sillimanite isograd. In addition, S_{1b} and S_3 generally dip away from the basin margin (fig. 7). These observations indicate that this protrusion of the margin has at some time affected these structures. The form surface of S_{1b} (fig. 11) shows few folds, because the surface is dipping shallowly. The S_{1b} form surface shows the axial traces of the folds trend northeast along the coast, similar to the trend of the calculated fold axes. Farther inland, where the calculated fold axes parallel the basin margin, the folds are less apparent on the form surface map. The form surface of S_3 (fig. 12) shows the F_4 folds in greater relief than the S_{1b} surface, because the S_3 surface dips more steeply to the north. Again the axial traces of these folds are similar in orientation to the calculated fold axes. When the S_{1b} and S_3 form surface maps are superposed, a marked difference in foliation orientation becomes apparent around Stook Hill (fig. 13, see also fig. 7). This divergence of the two foliations indicates a large-scale F_3 hinge because a folded foliation (S_{1b}) and an axial planar foliation (S_3) should be essentially parallel along limbs of tight to isoclinal folds and should be at a high angle to each other in the hinge of the fold. This possibility was indicated earlier by the shape of the small F_3 parasitic folds on the cross section and the large synformal hinge shown on the west end of the east-west cross section (fig. 9A).

F_3 and F_4 fold axes were calculated by taking the data points defining the hinges on the cross sections, plotting these strikes and dips on a stereonet, and finding the intersection of the planes. F_3 fold axes are plotted on the stereonet and on the map in figure 11. Although some of the spread in the data results from subsequent folding by F_4 (as seen in the cross section), the fold axes also change orientation in a progressive manner, from east to west, across the study area. Along the coastline, the F_3 fold axes generally trend north-northeast to northeast with most northeast (fig. 11). Along the western margin of the study area, the fold axes generally trend almost east. These differences in fold axis orientation between areas are reflected in the spread of S_{1b} poles on stereonets for the individual areas (fig. 7).

The F_4 fold axes were calculated from actual transects of data taken in the field for the purpose of defining the fold axes, as well as from data defining hinges on the cross sections. The fold axes are plotted on the stereonet and map in figure 12. The scatter of the F_4 axes occurs for

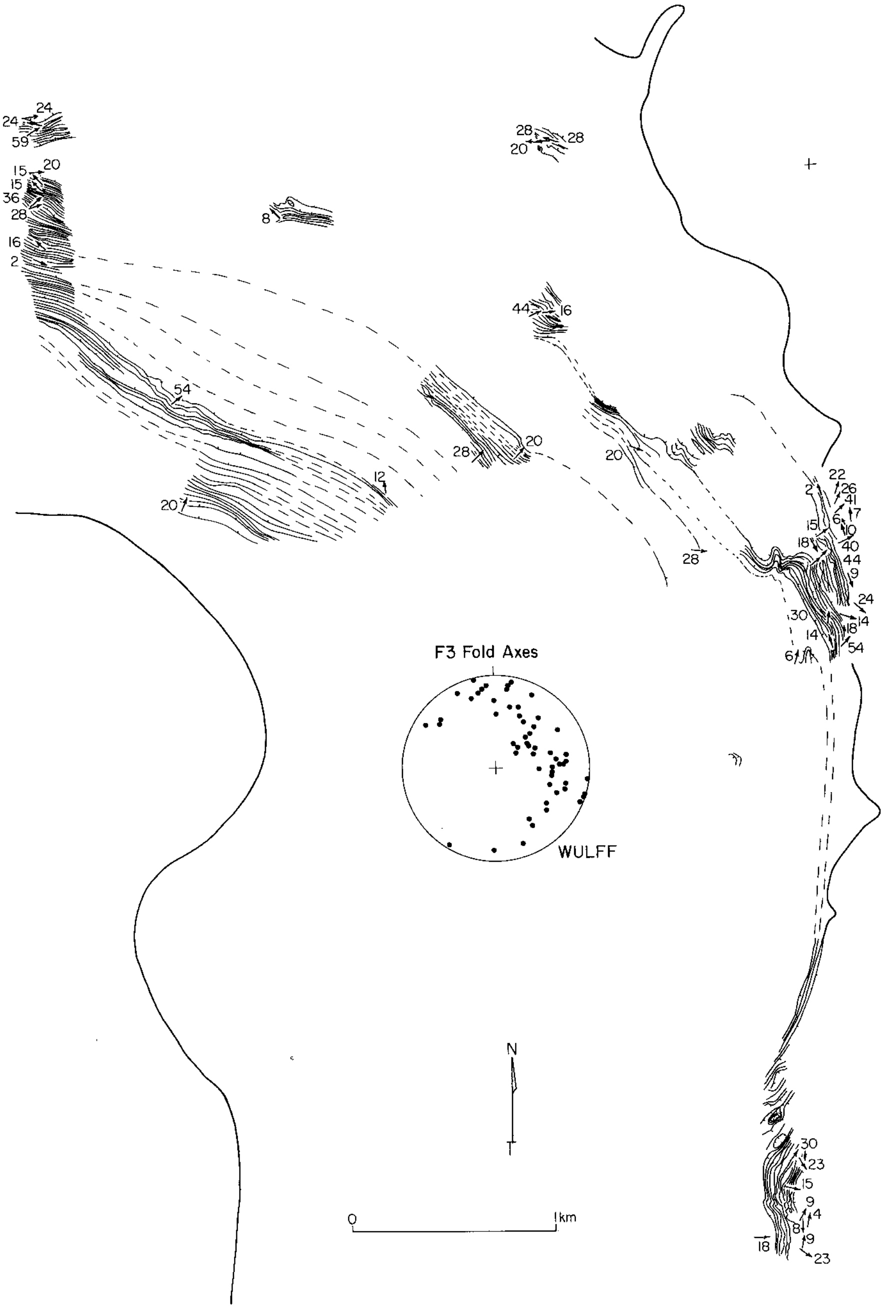

Fig. 11. Form surface map of S_{1b} with calculated F_3 fold axes superposed. The surface curves parallel to the basin margin (thick, solid line on far left). The fold axes change orientation across the study area, from northeast along the coast to almost east (east-northeast to west-northwest) along the western edge of the study area. A line of 400 m connects 6 to 8 measurements. Stereonet shows F_3 fold axes calculated from strike and dip data. Coastline (thick line on far right) is omitted for clarity where form surfaces come from coastal outcrops; if drawn, the coastline would parallel the eastern extent of the form surface lines.

Fig. 12. Form surface map of S_3 with measured and calculated F_4 fold axes superposed. The surface again curves, but the change in trend is 3 km east of the curve in the basin margin (solid line on far left). The folds stand out in greater relief than in figure 11, because the surface is dipping at a steeper angle. The F_4 fold axes also change orientation across the study area from northeast along the southern coast to northerly farther north and inland; variable north- and northeast-trends are observed, and northwest-trends occur, in addition, near the western margin of the study area. Stereonet shows F_4 fold axes measured in the field and calculated from strike and dip data. Coastline (thick line on far right) is omitted for clarity where form surfaces come from coastal outcrops; if drawn, the coastline would parallel the eastern extent of the form surface lines.

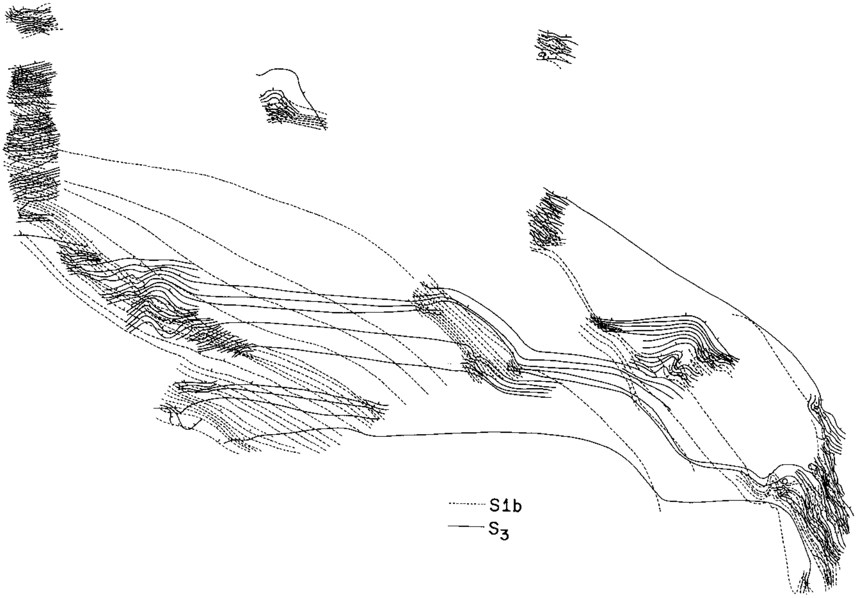

Fig. 13. Upper portion of S_{1b} (dashed lines) and S_3 (solid lines) form surface maps superposed. Foliations are parallel along the entire coast including the area not shown. Foliations are at a high angle inland, indicating a large F_3 fold hinge near Stook Hill (left side). The two foliations will be at a high angle near the hinge and subparallel along the limbs. Both surfaces are shown by continuous lines for clarity.

several reasons (illustrated in fig. 14): (1) The axes of the box folds observed on the cross sections are not coaxial and create an east-west spread. (2) F_4 is affected by later boudinage with a north-south extension direction which changes the orientations of the axes in a north-south direction. (3) The orientation of the F_4 fold axes changes progressively across the study area, as did F_3. Along the southern coastline (fig. 12), the F_4 axes trend northeast and become more northerly to the north. Farther inland, they have variable north- to northeast-trends, and along the western edge of the study area, northwest-trending fold axes (commonly one axis of a box fold) are also observed. Again the stereonet data for different areas (fig. 7) are consistent with these fold axes.

To summarize the history of deformation as determined by the geometric analysis: F_{1a} folds are large-scale, isoclinal, recumbent folds of bedding (S_0) with smaller parasitic folds on the limbs. F_{1b} folds are isoclinal with a shorter wavelength and fold the S_{1a} and S_0 surfaces. F_3 folds of S_0 and S_{1b} surfaces are presently isoclinal to open and recumbent to nearly upright and appear to verge to the south or west. Those seen in cross section are actually parasitic on a larger F_3 fold, the hinge of which was delineated by superposing form surface maps. The F_3 fold axes range in orientation from north-northeast to northeast along the coast to east

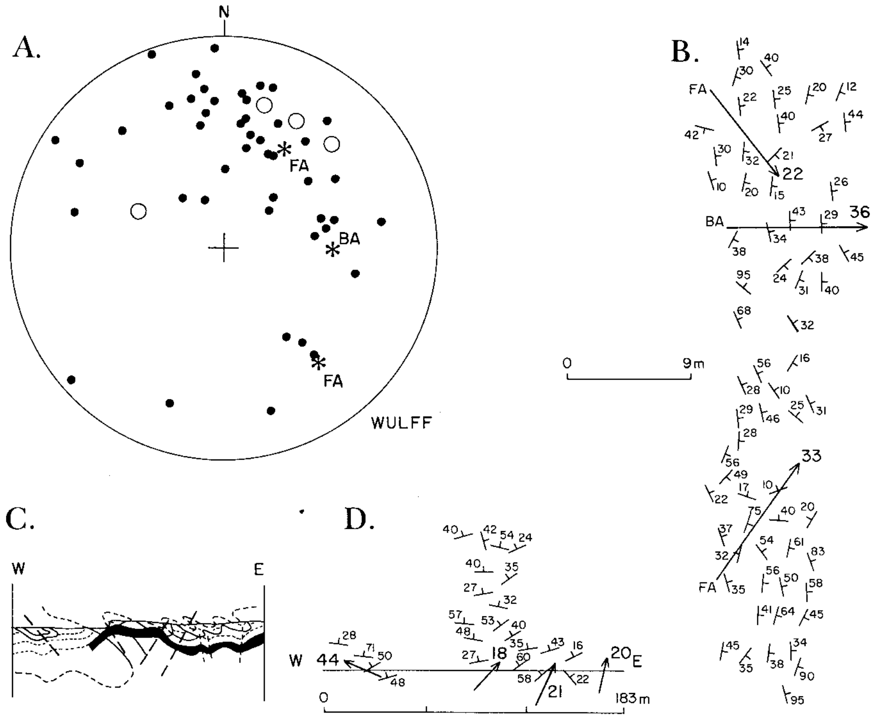

Fig. 14. Effects of boudinage and box folding on F_4. (A) Stereonet of F_4 data (*'s refer to axes shown in B; FA-fold axes, BA-boudin axes. Open circles refer to fold axes shown in D). (B) Map of part of coastline showing S_3 data, measured fold axes, and a boudin axis, observed in the field to affect the fold axes. These three axes are indicated on the stereonet in (A) by *'s and show that the north-south spread in F_4 axes is the result of boudinage. (C) Part of the east-west cross section near Stook Hill (fig. 9A) showing a box fold (highlighted). (D) Map of same area with S_3 data and F_4 fold axes. S1b shown on cross section has been omitted for clarity. These F_4 folds are indicated on the stereonet in (A) by open circles and show that the box folds help create the east-west spread in data points.

along the western edge of the study area. S_{1b} and S_3 surfaces parallel the curved basin margin. F_4 folds form large-scale, open box folds of S_3 that become tighter and shorter in wavelength toward the west. The fold axes trend northeast to north, with some additional northwest-trending axes in the western section of the study area.

DISCUSSION

Relationship of structural generations across the southern basin.—Correlation of structural generations across the southern portion of the Narragansett Basin is difficult, in part, because metamorphic grade changes abruptly, and conditions range from lowest greenschist to upper amphibolite facies. The earliest structural generations are sufficiently similar in expression to allow correlation, but the later structures are significantly different in character. Below we compare the structures in the present study area to those in three areas (see fig. 2 for locations): (1) the adjacent area immediately to the south (hereafter referred to as the Bonnet Shores area), where rocks are at biotite grade (Reck and Mosher, 1989; this area and the present study area together form the southwestern portion of the basin); (2) the south-central portion of the basin where rocks are almost exclusively garnet to staurolite grade (Beaverhead, Conanicut, Dutch, and Gould Islands; Burks, ms; Henderson, ms; Mosher and Berryhill, 1991; Mosher, unpublished data); and (3) the southeastern portion of the basin where the rocks are mainly chlorite to biotite grade (the eastern mainland, Aquidneck and Prudence Islands; Mosher, ms, unpublished data; Thomas, ms; Farrens, ms).

The first deformation (D_1) in the Bonnet Shores area and in the south-central portion of the basin is represented by two generations of isoclinal folds, F_{1a} and F_{1b}, and associated axial planar foliations, S_{1a} and S_{1b}, similar to those within the present study area. Both fold and cleavage generations and the interference pattern of the two can be seen in outcrop and mapped in these other areas. Only one generation of F_1 folds with an associated penetrative S_1 foliation has been documented in the lower grade southeastern portion of the basin. However, an earlier, poorly developed S_{1a} foliation has been observed at many localities. F_{1b}'s and F_1's (undifferentiated) outside the present study area, where later folds do not affect their orientations, show a westward vergence and have north-northeast-trending axes. The original vergence for F_{1a} folds cannot be determined.

The timing of early, Barrovian metamorphism (M_1) in the Bonnet Shores area and the south-central portion of the basin is similar to that for the present study area. Metamorphism began during the formation of S_{1a}, and the peak of metamorphism was synchronous with and postdates the formation of S_{1b}. In the southeastern portion of the basin, the peak of metamorphism postdates the first generation structures. The temporal relationship of the peak of metamorphism to the second generation of structures varies between syn- to pre-D_2 in that portion of the basin.

Second generation structures in the present study area are similar to those in the Bonnet Shores area and the south-central portion of the basin but differ from those in the southeastern portion of the basin. In the southeast, F_2 folds are regional- to outcrop-scale, open, north-northeast-trending, east-verging folds. A penetrative crenulation cleavage of S_1 is axial planar to these folds. In the south-central basin and in the Bonnet Shores area, only the crenulation cleavage is found, but the cleavage is unambiguously overprinted by the third and fourth generation structures (Henderson, ms; Reck and Mosher, 1989). In the Bonnet Shores area, two sets of clockwise-younging crenulations are found similar to those observed for the present study area. These structures are found all along the coastline from Plum Beach to Bonnet Shores (fig. 2), making a strong case for correlation of S_2 between the present study area and the Bonnet Shores area.

The most significant difference across the basin is in the third generation structures. In the southeastern portion of the basin, third generation structures are rare and occur locally along the southeastern basin margin. In the south-central portion of the basin, third generation structures formed at chlorite grade and occur in numerous discrete, north- and northeast-trending, sinistral transcurrent shear zones. Structures include: en echelon folds; east- and northeast-trending, open, chevron and box folds within northeast- and north-northeast-trending zones, respectively; superposed, noncoaxial folds and crenulation cleavages that young in a clockwise direction and are in an appropriate orientation to have formed as a result of progressive rotation in a sinistral noncoaxial strain field; sheath folds; tension gashes; and north-trending faults with sinistral offset (Mosher, 1983; Henderson, ms; Burks, ms; Mosher, Burks, and Reck, 1987; Mosher and Berryhill, 1991). Rather abruptly in the southwestern basin, D_3 forms a pervasive, metamorphic foliation that is axial planar to both mesoscopic and megascopic isoclinal, presently recumbent, folds. The presence of biotite and muscovite parallel to S_3 indicates that temperatures were still elevated. These F_3 and S_3 structures are not observed in the adjacent Bonnet Shores area (biotite grade). Instead, an east-trending crenulation and rare east-trending folds overprint the S_2 crenulation cleavage; no metamorphic minerals are associated with these structures.

Pervasive third generation structures have been documented in adjacent areas by other workers, but insufficient information was available to put these structures into any context. Thomas (ms) recognized a weakly developed late schistosity oriented N70°E 20°NW on Hope Island just north and east of the study area in the western passage of the Narragansett Bay (fig. 2) but found no such foliation on Prudence Island just to the east. Dreier (ms) also documented a late phase of Alleghanian folding with an axial planar crenulation cleavage in the Precambrian Blackstone Series north of the study area and adjacent to the western basin margin (fig. 1). These folds post-date first generation Alleghanian structures and trend east. She suggests that F_3 and S_3 may be localized along north-northwest-, north-, and northeast-trending faults.

Fourth generation structures are also different in character. In the south-central portion of the basin, fourth generation structures are generally restricted to the northeast-trending Beaverhead shear zone (figs. 1, 2). The structures include: dextral shear zones that reorient all previous structures (including sinistral shear zones and associated structures) into a northeast orientation; en echelon folds; north- to northeast-trending, open folds within northeast-trending shear zones; superposed, noncoaxial folds and crenulation cleavages that young in a counterclockwise direction and are in an appropriate orientation to have formed as a result of progressive rotation in a dextral noncoaxial strain field; kink bands; tension gashes; boudinage with a north-south extension direction; and northeast- to east-northeast-trending faults with a dextral offset (Mosher, 1983; Burks, ms; Mosher and Berryhill, 1991). In the southeastern portion of the basin, only boudinage with a north-south extension direction is observed (Farrens, ms; Mosher, 1983). In contrast, fourth generation structures in the southwestern portion of the basin are large-scale, open folds that fold all previous structures. Individual F_4 folds can be traced from the present study area into the Bonnet Shores area proving they are equivalent structures. In the Bonnet Shores area, these folds postdate intrusion of the Narragansett Pier Granite, whereas S_2 crenulations predate and D_3 structures appear to be concurrent with the intrusion (Reck and Mosher, 1989).

If a one to one correlation of the structural generations across the entire basin is made, the differences between the later structures must be explained. F_1 folds in the southeastern portion of the basin are most likely F_{1b} folds elsewhere. The poorly developed nature of the S_{1a}/F_{1a} structures reflects the low metamorphic grade which is not conducive to preservation of multiple generations of structures. The S_2 crenulation cleavages in the southwestern and south-central portions of the basin may correlate with the F_2/S_2 structures farther east. In the south-central portion of the basin, regional F_2 folds, if present, probably would not be recognized because of the numerous sinistral and dextral shear zones and the paucity of other outcrop. Regional, open F_2 folds, if present in the southwestern portion of the basin, might be obscured by the more dominant F_3 and F_4 folds. The correlation of F_3/S_3 in the present study area and F_4 folds in all the southwestern basin with D_3 and D_4 structures elsewhere is more problematic. The pervasiveness of the F_3 in the present study area and F_4 folds in all the southwestern basin could reflect: (1) deformation within many small shear zones whose boundaries are not seen because of the paucity of outcrop or (2) more widely distributed transcurrent shearing in an area proximal to a major shear zone or bounded by major zones such as the one in the western passage of the Narragansett Bay (Mosher and Berryhill, 1991). A bedrock elevation contour map (Reck, ms) for the southwestern portion of the basin shows a pronounced, narrow, linear low that bifurcates where the margin curves to the west (fig. 2). This lineament, as well as the basin margin, could also represent a major basement fault along which transcurrent shearing occurred. Both possibilities are supported by the occurrence of similar structures on Hope Island and within the Blackstone Series. The possibility of more widely distributed shearing is supported by the higher metamorphic grade of the rocks at the time of deformation and the abundance of massive metasandstones and metaconglomerates in the area. The rocks involved in the discrete shear zones in the south-central portion of the basin were at chlorite grade during that deformation and are primarily phyllites. Thus, the strain may have been partitioned into discrete zones, whereas in higher grade, more competent rocks, the strain may have been more widely distributed.

An alternative correlation of structural generations across the basin is possible. The F_3/S_3 structures could be part of the progressive S_{1a}/F_{1a}, F_{1b}/S_{1b} series for which increasingly more folds and foliations are preserved as the metamorphic grade increases westward. This relationship is suggested by the formation of the metamorphic fabric (S_3) and the apparent recumbent, isoclinal, and west-vergent nature of these structures. The presence of S_2 crenulations overprinted by S_3 suggests this correlation is not correct, but such overprinting is not common in the present study area. Possibly some crenulation of S_{1b} could have occurred locally before F_3/S_3 and be unrelated to F_2 folds in the southeastern portion of the basin. For this correlation, D_3 structures observed within shear zones elsewhere in the basin would be absent in the southwestern portion of the basin.

If the above correlation is made, F_4 folds could represent continued shortening. However, they are distinct from F_2 folds farther east as demonstrated by Reck and Mosher (1989) in the Bonnet Shores area. Thus in this scenario, F_4 folds (like F_3/S_3) would not have correlative structures in the south-central or southeastern portions of the basin. F_4 folds are very similar in style, scale, and timing to folds within the Beaverhead shear zone, making correlation with other D_4 structures a plausible alternative. The likelihood of the different correlations will be discussed below.

Effect of basin margin.—Although the basin margin is mapped in some places as a high angle fault or unconformity (nearly always modified by faults), most of the present basin margin is not exposed. The basin has been considered an erosional remnant of a much larger basin that extended across much of the Boston Platform (Quinn and Oliver, 1962; Grew, 1976; Skehan and others, 1979), suggesting that the present shape is the result of erosion. This study has shown that at least the curved, west-northwest-trending part of the southwestern basin margin is a significant feature, which influences the geometry of the structures. Geometric analysis shows that bedding (S_0), S_{1a}, S_{1b}, and S_3 foliations and the sillimanite isograd strike parallel to and dip away from this west-northwest-trending basement margin. This nearly east-strike and north-dip is in marked contrast to all other exposures throughout the entire southern portion of the Narragansett Basin. Everywhere else, bedding, foliations, and, for the most part, isograds strike north and dip either east or west. The effect of this west-northwest-trending margin is only observed in the 7 km^2 (3 km east, 2.3 km north) area adjacent to the margin. Within 0.2 km of the northern boundary of the present study area, bedding and foliations are again north-trending.

The apparent vertical deflection of the sillimanite isograd indicates uplift of the adjacent basement after the peak of metamorphism and therefore after S_{1b}. Bedding, S_{1b}, and probably S_{1a} (little data) curve following the trend of the basin margin, and their orientations could be explained by passive rotation during later uplift of this basement block by tectonic or erosional processes. The S_3 foliation does not curve following the basin margin trend. Instead, the change in strike from east to north is located 3 km east of the change in trend of the basin margin (fig. 12). Thus, S_3 foliations were not passively rotated into their present positions by later uplift. A highly speculative possibility is that the entire basin margin, along with the S_{1b}, S_3, and isograd surfaces, was folded by large northeast-trending folds. This idea would require folding of the basement in southwestern Rhode Island. Although it has been implied that the Hope Valley shear zone might be folded (O'Hara and Gromet, 1985; Reck and Mosher, 1989), the present data are insufficient to support such regional-scale folding. Further mapping of the basement between the basin and the Lake Char/Honeyhill fault is required to test this hypothesis. The most likely possibility is that the present basin margin shape existed during the formation of S_3 and influenced the orientation of S_3/F_3 and later structures. The third generation structures do not constrain the timing of the basement block uplift indicated by the isograd, as long as the margin was curved during their formation. However, uplift before or during D_3 is the most compatible with the resultant structures. If the growth of sillimanite resulted from rapid decompression after S_{1b} formation and prior to intrusion of the Narragansett Pier Granite, as proposed by Jones (ms), then uplift of this area would mark the change from convergence to transcurrent motion in the rest of the basin.

Evaluation of possible tectonic histories.—Possible tectonic histories that would explain the presence of the late phase folds (F_3 and F_4), in particular the variation in fold axis orientations, in the southwestern portion of the basin include crustal shortening (or extension) with a southwesterly direction of transport for F_3, crustal shortening for F_4, and transcurrent shearing for both F_3 and F_4. Below we will discuss each of these possibilities.

The possibility that F_3/S_3 is part of the early progressive deformation is constrained by the effect of the basement margin. If the present day margin shape already existed (as concluded above), the transport direction would need to be toward the southwest to explain the change from westward vergence near the north-trending basin margin to southward vergence near the west-northwest-trending margin. However, most F_3 fold axes plot in the northeast quadrant of the stereonet (fig. 11), making transport toward the southwest possible only if they are sheath folds or folds that have been reoriented into the transport direction. No evidence for sheath folds, rotation of fold axes, or high shear strains has been found in the present study area. The excellent preservation of sedimentary structures in the sandstones and conglomerates (including detrital quartzite clast shapes in sandstones) and of the F_{1b} folds argues against such high shear strains. More importantly, the basin margin could not have formed a rigid buttress over which the rocks were thrust, because the change in curvature of the margin does not correspond with that of S_3 (as discussed above), which it should if the two were genetically related in this manner. The same arguments preclude these structures being part of a later, separate phase of deformation associated with widely distributed, low-angle extensional shearing.

F_4 folds are effected less by the curved basin margin. A new orientation of F_4 folds occurs adjacent to the west-northwest-trending basin margin in addition to the orientations observed along the coast. Hence, these folds most likely formed after the basin margin had its present shape. F_4 folds could be explained by east-west shortening. The north-trending F_4 folds and the northeast- and northwest-trending ones could form synchronously if the latter two represent noncoaxial axes of box folds. However, the northeast-trending axes are much more common than the northwest-trending ones, and the northwest-trending ones seem to be localized near the western basin margin. This localization coupled with the apparent shift from northeast- to north-trending fold axes northward along the coast suggests that the evolution of these folds is more complex. Thus, crustal shortening does not explain adequately either F_3/S_3 in the present study area or F_4 in the southwestern basin.

Late-stage dextral shear zones have been documented within the adjacent basement (O'Hara and Gromet, 1985; Getty and Gromet, 1988), and both dextral and sinistral zones have been documented within the basin (Mosher, 1983; Burks, ms; Mosher and Berryhill, 1991). Thus transcurrent motion is a likely cause for the late phase structures in the southwestern portion of the basin. Unfortunately, unlike the south-central portion of the basin, kinematic indicators and discrete shear zones cannot be identified in the present study area. Hence, only the structural geometry can be used to try to reconstruct the kinematic history. For both F_3 and F_4 folds, transcurrent motion must generally produce north- to northeast-trending folds. Only two orientations and senses of motion do so (fig. 15): (1) north-trending sinistral transcurrent zones would result in northeast-trending folds that with further strain would rotate into north-trends; (2) northeast-trending dextral transcurrent zones would result in north-trending folds that would rotate into northeast-trends. In each of these cases, the west-northwest- to northwest-trending part of the margin might be reactivated. For the north-trending sinistral zone, the west-northwest-trending margin would undergo dextral riedal shearing producing east-northeast-trending folds that rotate into west-northwest-trends. For the northeast-trending dextral zones, the west-northwest-trending margin would undergo sinistral motion, which would produce north-northwest-trending folds that would rotate into west-northwest-trends. Thus, a north-trending, sinistral transcurrent zone would form folds compatible with F_3 folds, and a northeast-trending, dextral zone would form folds compatible with the F_4 folds. These zones are in the same orientation as the D_3 sinistral zone documented for the western passage of the Narragansett Bay (Mosher and Berryhill, 1991) and the Beaverhead shear zone (Mosher, 1983, Burks, ms) (fig. 2). Such motion requires that the basin margin have its present shape and behave rigidly with respect to the basin metasediments. The massive nature of the gneissic basement as compared to the well-foliated, interlayered schists and sandstones should have created a sufficient rheological contrast.

The conclusion that the F_3/S_3 structures are related to sinistral transcurrent motion and that the F_4 structures are related to dextral

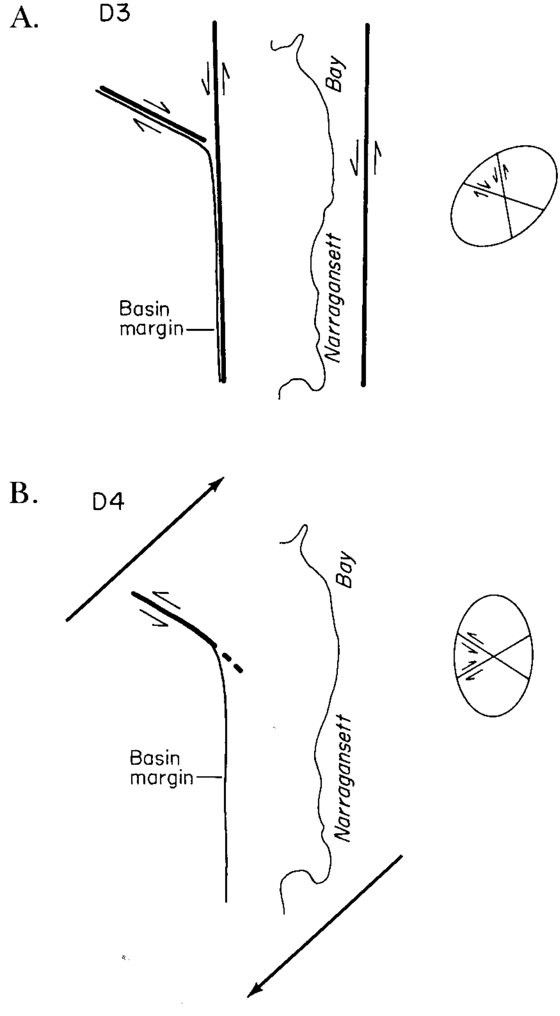

Fig. 15(A) D_3 sinistral shearing on north-trending zones: one in the western passage of the Narragansett Bay and one reactivating the north-trending basin margin. (Margin drawn slightly separate from faults for clarity.) The west-northwest-trending basin margin is reactivated as a dextral R′ riedal shear. This sense and orientation of shearing explain the change in fold axis orientations in figure 11. The incremental strain ellipse (ellipticity exaggerated) for a north-south oriented sinistral shear couple and the orientation of riedal shears is shown. (B) D_4 dextral shearing by northeast-trending shear couples reactivates the west-northwest-trending basin margin as a sinistral R′ riedal shear. The north-trending basin margin remains inactive. This model creates the pattern of fold axis orientations seen in figure 12. Early-formed fold axes would parallel the long axis of the strain ellipse. The incremental strain ellipse (ellipticity exaggerated) and the orientation of riedal shears for a northeast-trending dextral shear couple are shown.

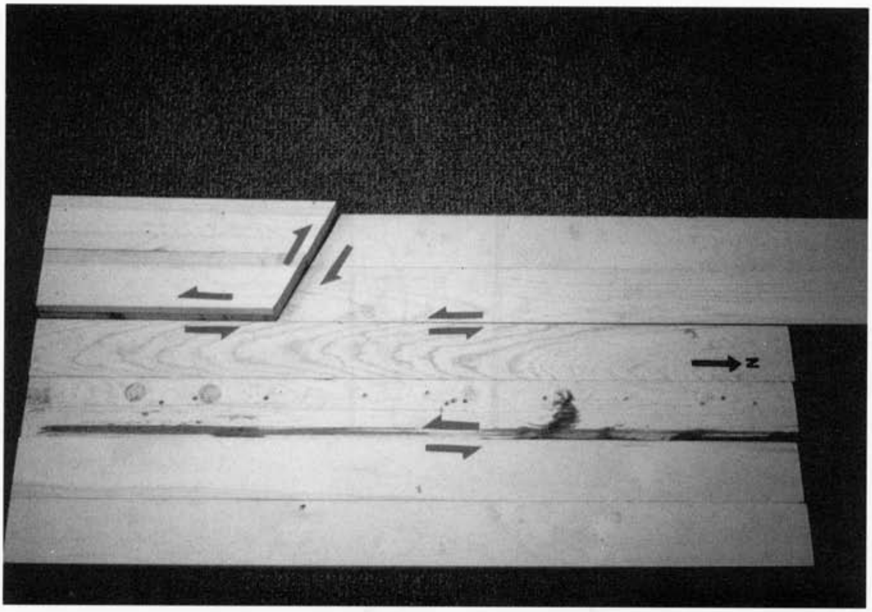

Fig. 16. Boards forming base of model. The long edges are oriented north, parallel to the postulated shear zone. The basin margin protrusion is the higher board. One shear zone represents the zone east of the study area in the western passage of the Narragansett Bay. The other is the reactivated north-trending basin margin. The west-northwest-trending basin margin is shown reactivated as an R′ riedal shear.

motion is supported by the data from the rest of the basin discussed previously. The identical overprinting relationships and similar styles of structures (except for F_3/S_3) between the present study area and adjacent Bonnet Shores area indicate that those structures are correlative. The orientation of many F_3's and the position of F_3/S_3 in the structural sequence suggest they also are correlative with the S_3 Bonnet Shores structures. Furthermore, correlation of S_2, S_3, and F_4 in the Bonnet Shores area with F_2/S_2, F_3/S_3, and D_4 structures elsewhere in the basin on the basis of the temporal relationships with the Narragansett Pier Granite (Reck and Mosher, 1989) supports a one to one correlation of structures across the basin.

Physical model.—To illustrate that the preferred combination of senses of shear and shear zone orientations would actually create the observed pattern of fold axes, two simple physical models were created. For F_3 folds, three wood boards were lined up with their edges parallel to the postulated north-trending sinistral shear zones (fig. 16). A fourth, thicker board, with its edge cut to match the basin margin, was used to represent the basement high. A piece of material was laid over the model and secured with tape down the centers of the boards to simulate the S_{1b}

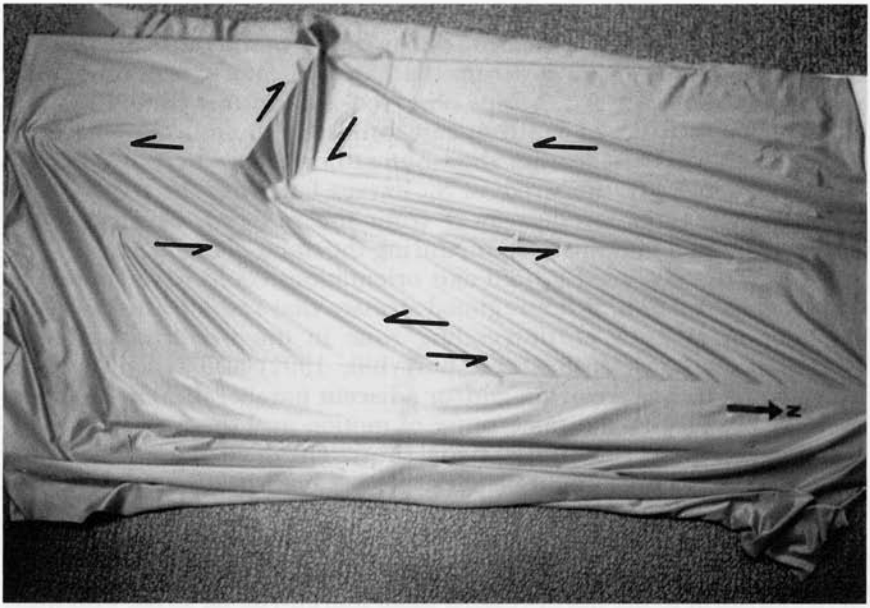

Fig. 17. Board and cloth model, after north-trending sinistral shearing and dextral R′ riedal shearing has been added, showing northeast-trending folds in the east resulting from north-south sinistral shearing and east-west fold axes in the west resulting from dextral R′ riedal shearing along the northwest-trending basin margin. In the west, the folds return to a more northeast orientation away from the boundary effects of the west-northwest-trending basin margin

surface. The boards were then moved to recreate the appropriate sense of strike-slip motion (fig. 17). The deformation was carried out in two steps. First, the north-trending sinistral movement was performed on both zones. Motion on the board representing the shear zone in the western passage of the Bay created the northeast-trending fold axes along the coast. Motion reactivating the north-trending basin margin created fold axes off the basement high that trend northeast as well but plunge more steeply than those farther east. The dextral R′ riedal shear was then added. Motion reactivating this west-northwest-trending basin margin created the east-trending fold axes.

The pattern of fold axes created by both movements on the model matches the observed pattern very well (fig. 11), with northeast-trending, shallowly plunging fold axes along the coast, northeast-trending, steeper plunging fold axes closer to the basin margin, and nearly east-trending fold axes adjacent to the west-northwest-trending margin. Some northeast-trending folds are observed near the west-northwest-trending margin in both the model and on the form surface map of S_{1b} (figs. 11, 17). The few northwest-trending folds on the map near the west-northwest-trending margin can be produced by continued shearing, causing east-trending folds to rotate into the shear zone. Shearing along an uplifted basement block (as in the model) or shearing during uplift would cause the rotation of the axial planes (S_3) away from the basement block, resulting in the northward and eastward S_3 dips observed around this curved margin. The change in strike of S_3 (from east to north) would occur where the effects of the riedal shearing died out rather than where the margin curved. In contrast, the strike of S_{1b} curves following the trend of the basin margin (and S_{1b} dips away from the margin), because it was passively rotated into this position during the uplift of the block.

Thus, the observed F_3 fold axis orientations could have formed by transcurrent motion, if the regional stresses that caused sinistral strike slip motion along a north-trending zone in the western passage of Narragansett Bay (Mosher and Berryhill, 1991) also reactivated the north-trending basin margin and/or adjacent parallel shear zone (lineament in fig. 2) with the same sense of motion and the west-northwest-trending margin as a dextral R′ riedal shear. The third phase of deformation in the study area might be pervasive because the area was bounded by two major shear zones. This idea is supported by the presence and location of third generation structures north of the study area (on Hope Island in western passage of Narragansett Bay and within the Blackstone Series adjacent to the northwestern basin margin) along strike with these two postulated zones. Another contributing factor to the widely distributed strain could be the somewhat elevated temperatures during deformation and the more competent nature of the rocks. This evidence suggests that D_3 is not a minor event at all, as previously thought, but is regionally significant and probably has reactivated other appropriately oriented faults in the region.

For F_4 folds, a wood and cloth model was used again to verify that the hypothesized deformation would create the fold axis pattern observed in the study area (fig. 18). The cloth was laid over a smooth surface and a thicker board to represent the basement high. First, two boards were used to create the northeast-dextral shear couple in a diffuse zone encompassing the southwestern portion of the basin. Minor motion caused north-trending folds that rotated to northeast-trends as shearing progressed. (Fig. 18 is an intermediate stage showing north-northeast-trending folds.) The basement high was then moved to create the sinistral R′ riedal shear along the west-northwest-trending basin margin. This motion resulted in northwest-trending folds near the west-northwest-trending margin, which gradually changed in orientation to north-trending folds away from this margin. During the first step of northeast-trending dextral shearing, northeast-trending folds formed near the west-northwest-trending margin but were almost totally removed by the second R′ riedal shearing step. When the reverse sequence was tried, the northwest-trending folds were lost and replaced by northeast-trending folds near the west-northwest-trending margin. When movement along both orientations was simultaneous, only one orientation of folds (those corresponding to the greatest displacement) prevailed. As rocks should

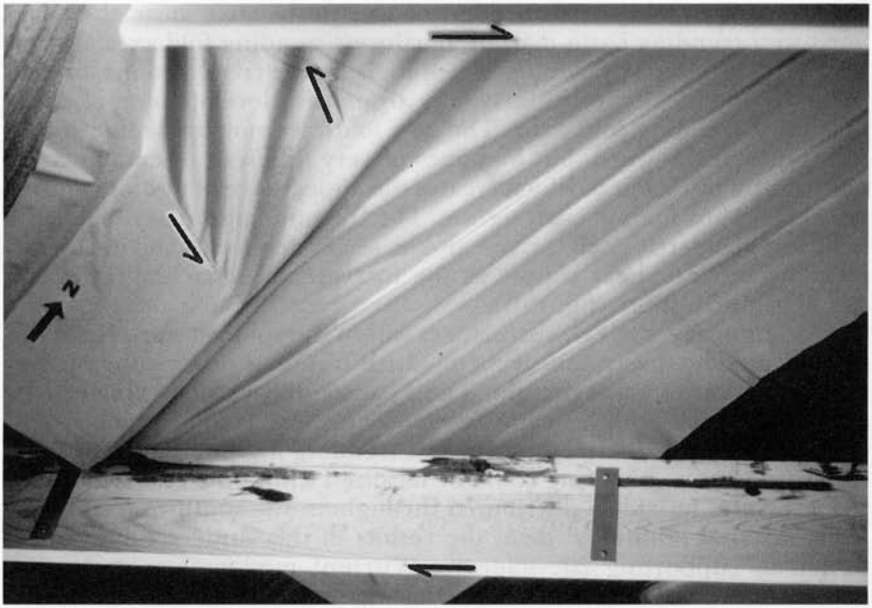

Fig. 18. Board and cloth model of northeast-trending D_4 dextral shearing distributed over a broad area and sinistral R′ riedal shearing localized along the west-northwest-trending basin margin. North-northeast-trending fold axes in the east gradually swing to north-trending approaching the western part of the basin. Northwest-trending fold axes are found in the west. See text for discussion.

be able to record both orientations, and motions should be simultaneous, one would expect both orientations in this area. The gradual swing in orientation from northwest- to northeast-trends observed in figure 18, going from the area near the west-northwest-trending margin toward the east, reflects the relative magnitudes of the two strains. Away from the west-northwest-trending margin, the dextral shearing was most intense, and fold axes formed with north-trends and progressively rotated clockwise to the northeast. Near the west-northwest-trending margin, most of the shear strain was accommodated by R′ riedal sinistral motion, so dextral-related folds that trend north to northeast reflect minor strains and interfere with northwest-trending folds related to the sinistral motion.

Again, the simulated pattern matches the observed pattern very well (figs. 12, 18). The F_4 fold axes trend north in the Bonnet Shores area, gradually change to northeast along the southern coast of the present area, and generally trend more northerly farther to the north—presumably reflecting a zone of higher shear strain in the center. Farther inland where the basin margin curves, most folds are north- to north-northeast-trending, although a few northeast-trending folds are found (fig. 12). Along the western edge of the study area, near the west-northwest-trending basin margin, northwest-trending fold axes also appear. The observed tightening of box folds on the cross sections, toward the west (fig. 9A), probably results from the development of these northwest-trending fold axes. The box folds are not tightening in the true sense of the word, but fold axes of very different orientations are intersecting more often, which creates the appearance of tighter, shorter wavelength box folds in cross section. The D_4 boudinage, described in the field and geometric analyses, can also be accounted for by the northeast-trending dextral shear couple as the incremental stretching direction would be north-south (fig. 15B).

In summary, the F_3/S_3 structures within the southwestern basin can be explained by sinistral shearing on north-trending zones with reactivation of the entire basin margin. The F_4 structures can be explained by dextral shearing with a northeast-trending shear couple which reactivates the west-northwest- to northwest-trending margin. For both F_3/S_3 and F_4 structures, shearing could be localized within discrete (but unobserved) zones or widely distributed throughout the southwestern basin. Thus, without additional data, the results of this study are best interpreted as supporting late-stage transcurrent motions similar to that demonstrated for the rest of the Narragansett Basin. The northeast-trending dextral shear couple postulated to explain the fourth generation structures in the study area has the same shear sense and orientation as that of the Beaverhead shear zone. However, the shearing has become more regionally penetrative and broadly distributed than that documented in the south-central portion of the basin. Thus, it is likely that the dextral transcurrent motion is more regional in scale and has reactivated the Beaverhead shear zone.

SUMMARY AND TECTONIC IMPLICATIONS

For a long time, the Alleghanian orogeny in southeastern New England was considered a "relatively minor" orogenic event of little regional significance (Rodgers, 1967). In recent years, the true magnitude of the deformation associated with the Alleghanian is being recognized. This study offers conclusive evidence that the early deformation within the Narragansett Basin resulted from collision-driven convergence. D_1, in the southwestern portion of the basin, represents a deep-seated collisional deformation resulting from west-directed tectonic transport as evidenced by the large-scale, recumbent, nappe-like F_{1a} and F_{1b} folds that formed concurrent with upper amphibolite facies metamorphism. The concept of deep-seated, high-grade collisional deformation during D_1 is corroborated by the concurrent formation of an S-type granite (the Narragansett Pier Granite) at depth. Other authors have also suggested deep-seated, high-grade Alleghanian deformation in the region (Murray, 1988; Wintsch and Sutter, 1986; O'Hara and Gromet, 1983, 1985). Although F_{1a} fold vergence cannot be determined, the vergence of F_{1b} and of F_1 folds where only one generation is present indicates thrusting of the metasediments westward out of the basin. This westward thrusting is opposite to that proposed by Wintsch and Sutter (1986) for eastern Connecticut and suggested, by them, for all of Rhode Island, including the Narragansett Basin. D_2 structures that are well expressed in the southeastern basin have an opposite transport direction suggestive of backfolding (Mosher, 1985), perhaps as eastern Rhode Island was affected by east-directed thrusting in eastern Connecticut. The effects of any regional D_2 in the southwestern basin have been obscured by later deformation.

The apparent regional importance of transcurrent motion with changing senses of motion and orientations with time is further supported by the present study. Our results, coupled with previous work (Mosher and Berryhill, 1991; Burks, ms), indicate that late-stage Alleghanian sinistral shearing in the western passage of the Narragansett Bay extends northward, penetratively affecting a wide area, and that the north-trending basin margin has been reactivated by sinistral shearing, quite possibly along its entire length, affecting the adjacent basement. These results strongly suggest that other north-trending faults in southeastern New England may have experienced unrecognized D_3 sinistral transcurrent motion. This study also demonstrates that D_4 is a regional event and is not just concentrated along the northeast-trending Beaverhead shear zone. The timing of this dextral motion is the same as that observed in the southern Appalachians along the Irmo and Brevard shear zones (Secor and others, 1986; Sinha, Hewitt, and Rimstidt, 1988).

Comparison of the dynamothermal histories of eastern Connecticut and western Rhode Island with that for the southern portion of the Narragansett Basin illustrates the diachronous nature of the Alleghanian orogeny. The dissimilarities between their tectonic evolution suggest that the two areas were decoupled during much of the late Paleozoic. However, the Devonian Scituate Granite extends from the Hope Valley shear zone (which deforms it) to the margin of the Narragansett Basin (fig. 1), negating the possibility of any later structural juxtaposition. The two regions must therefore represent much different structural levels. For example, recent investigations (Wintsch and Sutter, 1986; Gromet, 1991; Getty and Gromet, 1992a and b) indicate that during the Pennsylvanian, thrusting in eastern Connecticut and dextral shearing in western Rhode Island occurred at upper amphibolite facies conditions *while* the sediments were being deposited in the Narragansett Basin. One possible explanation is that underthrusting also occurred beneath the Narragansett Basin at the same time. If so, the basin could represent extensional collapse at the surface as a result of an overthickened wedge. Alternatively, oblique collision of Africa with North America during the Carboniferous may have forced part of southeastern New England northeastward causing sinistral strike slip motion (Geiser and Engelder, 1983; Sacks and Secor, 1990). In that case, the basin would represent a surficial pull apart basin (McMaster, de Boer, and Collins, 1980; Mosher, 1983). In either case, the subsequent dynamothermal, contractional deformation of the basin sediments undoubtedly reflects continued thrusting and progressive burial of the basin. Abundant evidence from the rest of the Appalachians indicates a shift from northwest- to west-directed motion of Africa relative to North America around 290 Ma (Geiser and Engelder, 1983; Mosher, 1985; Sacks and Secor, 1990). Such a shift is consistent with the timing of dextral motion on the Hope Valley shear zone (293 Ma; Gromet, 1991) and with cessation of sedimentation and the onset of west-directed deformation in the basin (Mosher, 1985).

Post-contractional deformation is again different in the two areas but must reflect a similar overall tectonic history. Although the intrusion of the Narragansett Pier Granite into the southwestern basin at 273 Ma occurred during extension related to sinistral transcurrent motion within the basin (Zartman and Hermes, 1987; Reck and Mosher, 1989), pressure estimates indicate that about 6 km of unroofing took place between the formation of S_{1b} and granite intrusion (Jones, ms). Thus the northwest-directed extension and thinning of an overthickened crust around 285 to 272 Ma documented for eastern Connecticut (Goldstein, 1989; Getty and Gromet, 1992a and b) probably also affected the area containing the basin. The presence of sinistral transcurrent motion within the basin simultaneous with northwest extension in nearby Connecticut suggests that, although the two areas were both responding to crustal thinning, the southeastern portion was still affected by interaction with the African plate. This interaction is even greater after 273 Ma, because the basin is affected by dextral northeast-trending shearing, similar to much of the southern Appalachians. The extension in eastern Connecticut may be related to a releasing bend in a pan-Appalachian dextral fault system as proposed by Goldstein (1989) or may represent continued extension unrelated to the dextral transcurrent motion. Crustal extension concurrent with dextral shearing has also been reported for the Kiokee belt of the southern Appalachian Piedmont (Snoke and Frost, 1990). The late-stage dextral motion within the Narragansett Basin and along the length of the Appalachians may reflect counterclockwise motion of Africa prior to extension during the late Triassic (Mosher, 1985; Sacks and Secor, 1990) as required by the plate reconstructions of McKerrow and Ziegler (1972).

ACKNOWLEDGMENTS

This paper was modified from a master's thesis done at the University of Texas at Austin. Financial support was provided by the Geology Foundation of the Department of Geological Sciences at the University of Texas at Austin and Sigma Xi. The Department of Geological Sciences further provided significant support by making all the thin sections used in this research. Mr. Peter Tauvers allowed the use of his stereonet program, NetCity. Early versions of this manuscript benefited from comments by Drs. W. D. Carlson, W. R. Muehlberger, B. H. Reck, D. P. Murray, M. T. Brandon, and one anonymous reviewer.

REFERENCES

Aleinikoff, J. N., Moench, R. H., and Lyons, J. B., 1985, Carboniferous U-Pb age of the Sebago batholith, southwestern Maine: Geological Society of America Bulletin, v. 96, p. 990–996.

Arthaud, F., and Matte, P., 1977, Late Paleozoic strike-slip faulting in southern Europe and northern Africa: result of a right-lateral shear zone between the Appalachians and the Urals: Geological Society of America Bulletin, v. 88, p. 1305–1320.

Burks, R. J., ms, 1981, Alleghanian deformation and metamorphism in southwestern Narragansett Basin, RI: M. A. thesis, University of Texas, Austin, 93 p.

——— ms, 1985, Incremental and finite strains within ductile shear zones, Narragansett Basin, RI.: Ph.D. dissertation, University of Texas, Austin, 164 p.

Dallmeyer, R. D., 1982, $^{40}Ar/^{39}Ar$ ages from the Narragansett Basin and southern Rhode Island basement terrane: Their bearing on the extent and timing of Alleghanian tectonothermal events in New England: Geological Society of America Bulletin, v. 93, p. 1118–1130.

Dreier, R. B., ms, 1985, The Blackstone Series: evidence for Precambrian Avalonian and Permian Alleghanian tectonism in southeastern New England: Ph.D. dissertation, University of Texas, Austin, 249 p.

Farrens, C. M., ms, 1982, Styles of deformation in the southeastern Narragansett Basin, Rhode Island and Massachusetts: M. A. thesis, University of Texas, Austin, 66 p.

Geiser, P. A., and Engelder, T., 1983, The distribution of layer-parallel shortening fabrics in the Appalachian foreland of New York and Pennsylvania: Evidence for two non-coaxial phases of the Alleghanian orogeny, *in* Hatcher, R. D., Jr., Williams, H., and Zeitz, I., editors, Contributions to the tectonics and geophysics of mountain chains: Geological Society of American Memoir 158, p. 161–175.

Getty, S. R., and Gromet, L. P., 1988, Alleghanian polyphase deformation of the Hope Valley shear zone, southeastern New England: Tectonics, v. 7, p. 1325–1328.

——— 1992a, Geochronological constraints on ductile deformation, crustal extension, and doming about a basement-cover boundary, New England Appalachians: American Journal of Science, v. 292, p. 359–397.

——— 1992b, Evidence for extension at the Willimantic dome, Connecticut: Implications for the Late Paleozoic tectonic evolution of the New England Appalachians: American Journal of Science, v. 292, p. 398–420.

Goldstein, A. G., 1989, Tectonic significance of multiple motions on terrane-bounding faults in the northern Appalachians: Geological Society of America Bulletin, v. 101, p. 927–938.

Grew, E. S., 1976, Pennsylvanian rocks of east-central Massachusetts, *in* Cameron, B., editor, Geology of southeastern New England (New England Intercollegiate Geologic Field Conference, 68th Annual Meeting, Boston, Massachusetts): Princeton, New Jersey, Science Press, p. 383–427.

Grew, E. S., and Day, H. W., 1972, Staurolite, kyanite and sillimanite from the Narragansett Basin of Rhode Island: U.S. Geological Survey Professional Paper 800-D, p. 151–157.

Gromet, L. P., 1991, Direct dating of deformational fabrics: Mineralogical Association of Canada, May, 1991, Short Course Handbook on Applications of Radiogenic Isotope Systems To Problems in Geology, chapter 5, p. 167–189.

Henderson, C. M., ms, 1984, South-central Narragansett Basin, Rhode Island: role of preexisting intrabasinal horsts and grabens in Alleghanian deformation: M. A. thesis, University of Texas, Austin, 47 p.

Henderson, C. M., and Mosher, S., 1983, Narragansett Basin, Rhode Island: role of intrabasinal horsts and grabens in Alleghanian deformation: Geological Society of America Abstracts with Programs, v. 15, p. 129.

Jones, D. E., ms, 1987, Phase equilibria and conditions of metamorphism in the southwest portion of the Narragansett Basin: M. S. Thesis, University of Rhode Island, Kingston, 210 p.

Lyons, P. C., 1984, Carboniferous megafloral zonation of New England, *in* Sutherland, P. K., and Manger, W. L., editors, Neuvieme Congres International de Stratigraphie et de Carbonfere, Compte Rendu, v. 2, Biostratigraphy: Carbondale, Illinois, Southern Illinois University Press, v. 2, p. 503–514.

Lyons, P. C., Tiffney, B., and Cameron, B. W., 1976, Early Pennsylvanian age of the Norfolk Basin, southeastern Massachusetts, based on plant megafossils, *in* Lyons, P. C., and Brownlow, A. H., editors, Studies in New England Geology: Geological Society of America Memoir 146, p. 181–197.

Mahler, J. P., ms, 1988, Late-stage Alleghanian wrenching of the Narragansett Basin, Rhode Island: M. A. thesis, University of Texas, Austin, 83 p.

McKerrow, W. S., and Ziegler, A. M., 1972, Palaeozoic Ocean: Nature, v. 240, p. 92–94.
McMaster, R. L., de Boer, J., Collins, B. P., 1980, Tectonic development of southern Narragansett Bay and offshore Rhode Island: Geology, v. 8, p. 496–500.
Miller, E. T., 1952, Inshore marine magnetic investigations: the area from New Jersey to Cape Cod, Mass: Geological Society of America Bulletin, v. 63, p. 1279.
Mosher, S., ms, 1978, Pressure solution as a deformation mechanism in the Purgatory Conglomerate, Ph.D. dissertation, University of Illinois, Urbana, 181 p.
——— 1983, Kinematic history of the Narragansett Basin, Massachusetts and Rhode Island: constraints on late Paleozoic plate reconstructions: Tectonics, v. 2, p. 327–344.
——— 1985, Effects of Alleghanian accretion of the Boston platform on the western Narragansett Basin, Rhode Island: Geological Society of America Abstracts with Programs, v. 17, p. 670.
Mosher, S., and Berryhill, A. W., 1991, Structural analysis of progressive deformation within complex transcurrent shear zone systems: southern Narragansett Basin, Rhode Island: Journal of Structural Geology, v. 13, p. 557–578.
Mosher, S., Burks, R. J., and Reck, B. H., 1987, Alleghanian deformation in the southern Narragansett Basin, Rhode Island, *in* Roy, D. C., editor, Northeastern Section of the Geological Society of America Centennial Field Guide, v. 5: Boulder, Colorado, Geological Society of America, p. 191–194.
Murray, D. P., 1988, Post-Acadian metamorphism in the Appalachians, *in* Harris, A. L., and Fettes, D. J., editors, The Caledonian-Appalachian orogen: Geological Society of London Special Publication 38, p. 597–609.
Murray, D. P., and Mosher, S., 1984, Permian deformation and metamorphism in southeastern New England: Geological Society of America Abstracts with Programs, v. 16, p. 53.
Mutch, T. A., 1968, Pennsylvanian nonmarine sediments of the Narragansett Basin, MA-RI: Geological Society of America Special Paper 106, p. 177–209.
O'Hara, K. D., and Gromet, L. P., 1983, Textural and Rb-Sr isotopic evidence for late Paleozoic mylonitization within the Honey Hill Fault Zone, southeastern Connecticut: American Journal of Science, v. 283, p. 762–779.
——— 1985, Two distinct late Precambrian (Avalonian) terranes in southeastern New England and their late Paleozoic juxtaposition: American Journal of Science, v. 285, p. 673–709.
Quinn, A. W., and Oliver, W. A., Jr., 1962, Pennsylvanian rocks of New England, *in* Branson, C. C., editor, Pennsylvanian System in the United States: Tulsa, Oklahoma, American Association of Petroleum Geologists, p. 60–73.
Reck, B. J. H., ms, 1985, Deformation and metamorphism in the southwestern Narragansett Basin and their relationship to granite intrusion: M. A. thesis, University of Texas, Austin, 76 p.
Reck, B. H., and Mosher, S., 1989, Timing of intrusion of the Narragansett Pier Granite relative to deformation in the southwestern Narragansett Basin, Rhode Island: Journal of Geology, v. 96, p. 677–692.
Rodgers, John, 1967, Chronology of tectonic movements in the Appalachian region of eastern North America: American Journal of Science, v. 265, p. 408–427.
Sacks, P. E., and Secor, D. T., Jr., 1990, Kinematics of Late Paleozoic continental collision between Laurentia and Gondwana: Science, v. 250, p. 1702–1705.
Secor, D. T., Jr., Snoke, A. W., Bramlett, K. W., Costello, O. P., and Kimbrell, O. P., 1986, Character of the Alleghanian orogeny in the southern Appalachians: Part I. Alleghanian deformation in the eastern Piedmont of South Carolina: Geological Society of America Bulletin, v. 97, p. 1319–1328.
Severson, R. H., ms, 1981, Depositional environments, facies relationships, and coal occurrence in Carboniferous sediments of the Narragansett Basin: M. S. thesis, University of Rhode Island, Kingston, 105 p.
Sinha, A. K., Hewitt, D. A., and Rimstidt, J. D., 1988, Metamorphic petrology and strontium isotope geochemistry associated with the development of mylonites: an example from the Brevard fault zone, North Carolina: American Journal of Science, v. 288-A, p. 115–147.
Skehan, J. W., Murray, D. P., Hepburn, J. C., Billings, M. P., Lyons, P. C., and Doyle, R. G., 1979, The Mississippian and Pennsylvanian (Carboniferous) Systems in the United States—Massachusetts, Rhode Island, and Maine: U.S. Geological Survey Professional Paper 1110-A, 30 p.
Skehan, J. W., Rast, N., and Mosher, S., 1986, Paleoenvironmental and tectonic controls of sedimentation in coal-forming basins of southeastern New England, *in* Lyons, P. C., and Rice, C. L., editors, Paleoenvironmental and tectonic controls in coal-forming basins of the United States: Geological Society of America Special Paper 210, p. 9–30.

Snoke, A. W., and Frost, B. R., 1990, Exhumation of high pressure pelitic schist, Lake Murray spillway, South Carolina: evidence for crustal extension during Alleghanian strike-slip faulting: American Journal of Science, v. 290, p. 853–881.
Snoke, A. W., and Mosher, S., 1989, The Alleghanian orogeny as manifested in the Appalachian internides, *in* Hatcher, R. D., Veile, G. W., and Thomas, W. A., editors, The Appalachian-Ouachita Orogen in the United States: Geological Society of America, v. F-2, p. 288–318.
Thomas, K. J., ms, 1981, Deformation and metamorphism in the central Narragansett Basin of Rhode Island: M. A. thesis, University of Texas, Austin, 96 p.
Wintsch, R. P., and Sutter, J. F., 1986, A tectonic model for the late Paleozoic of southeastern New England: Journal of Geology, v. 94, p. 459–472.
Zartman, R. E., and Hermes, O. D., 1987, Archean inheritance in zircon from late Paleozoic granites from the Avalon zone of southeastern New England: an African connection: Earth and Planetary Science Letters, v. 82, p. 305–315.
Zartman, R. E., Hermes, O. D., and Pease, M. H., Jr., 1988, Zircon crystallization ages, and subsequent isotopic disturbance events in gneissic rocks of eastern Connecticut and western Rhode Island: American Journal of Science, v. 288, p. 376–402.